Synthesis and Characterization of Gelatin-Shelled Microbubbles

by

Yibai He

A thesis submitted in partial fulfillment of the requirements for the degree of

Master of Science

in

Chemical Engineering

Department of Chemical and Materials Engineering

University of Alberta

Abstract

This study focuses on the synthesis process of gelatin-shelled microbubbles and their characterization. A new method to synthesize gelatin-shelled microbubbles was described. Briefly, Traut's reagent was used to thiolate gelatin molecules; then sonication forces were placed at the water-air surface of the gelatin solution to generate microbubbles. Thiolated gelatin molecules can form S-S bonds between each other, forming a shell encapsulating air. When gelatin's concentration is 5% w/v at pH 8, Traut's reagent is 20 times molar excess of gelatin, and sonication time and amplitude is 45sec and 25% respectively, the microbubbles have a diameter of 1107 nm with a shell thickness of about 175 nm. Among different experiment parameters that can affect the size of the microbubbles, sonication time and amplitude have the biggest impact; and both of them have a positive correlation with bubble sizes. Gelatin's concentration also has a positive correlation with bubble sizes, although it doesn't have as big an impact as the other two parameters. Solution pH doesn't have a clear impact on bubble sizes. When the ratio of Traut's reagent and gelatin is about 10 to 20, the size of microbubbles tends to be the largest. The functional groups on gelatin can retain their reactivity after forming the shell, making them able to bind various protein or DNA drug molecules.

Furthermore, a two-step method was studied using gelatin as an example, which increases the level of thiolation of gelatin. It was found that after gelatin is aminated with EDC and ethylenediamine, up to 8 times more thiol groups can be introduced onto the gelatin surface and potentially increase the shell stability. This two-step method can be especially useful for proteins that may not have many natural thiol and amine groups; and it can potentially provide the opportunities for loading many drug molecules that are previously impossible to be delivered by proteinaceous microbubbles.

Dedicated to my parents and my beloved grandma

Acknowledgements

I'd like to sincerely thank Dr. Qingxia Liu, who is not only my supervisor but more importantly a mentor in my life. He guided me through my experiments and research, and also gave me life advice and encouragement when I was at my lowest point. I am forever grateful to have him as my supervisor.

I'd like to sincerely thank my therapist Ms. Sonia Zimmerman, who has helped me tremendously in my battle against mental health issues and guided me through difficulties in life patiently.

I'd like to thank everyone in my group, for all the training and discussions. I'd like to thank Dr. Shiau-yin Wu in nanofab and Dr. Ni Yang for their help in training me to use the equipment and always answering my questions.

I'd like to thank my family for their continuous support and unconditional love.

I'd like to thank everyone in my life for their positive influence.

Table of Contents

List of Figures

List of Symbols

I_t	Transmitted intensity
I_0	The intensity of the original light beam
A	Absorbance
ε	Absorption coefficient
l	Path length
c	concentration
R_H	Hydrodynamic radius
D	Translational diffusion coefficient
k_B	Boltzmann's constant
T	Temperature
η	Viscosity
Δf	Frequency change
Δm	Mass change
n	Overtone number
Δp	Pressure difference
γ	Surface tension
R	The radius of the bubble

List of Abbreviations

MB	Microbubbles
EWP	Egg white protein
BSA	Bovine serum albumin
w/v	Weight per volume concentration
ELISAs	Enzyme-linked immunosorbent assays
FE-SEM	Field emission scanning electron microscopy
DLS	Dynamic light scattering
QCM	Quartz crystal microbalance
PBS	Phosphate-buffered saline solution
EDC	1-ethyl-3-(3-dimethylaminopropyl) carbodiimide
EDTA	Ethylenediaminetetraacetic acid
FTIR	Fourier-transform infrared spectroscopy
TNB	5-thio-2-nitrobenzoate
DTNB	5,5'-dithio-bis-(2-nitrobenzoic acid)

Chapter 1 Introduction

1.1 Background

Microbubbles are small gas microspheres that typically have a diameter of under 10 micrometres. Because of their suitable sizes and acoustic properties, many studies have been conducted to understand how to use them in different areas, including ultrasonic imaging, drug delivery, and particle removal. However, a lot of challenges remain around microbubbles, including their short lifespan and low stability. Various materials such as proteins, lipids, surfactants, and polymers have been used as shells to improve the stability of microbubbles; and some of them have achieved good results in controlling the bubble size and stability. But in the case of protein shells, only a few proteins have been used as the shells to make stable microbubbles successfully. It's important to explore other protein shells to expand the drug loading capabilities of microbubbles; and gelatin is a great candidate because of its favourable properties such as low toxicity, high biocompatibility and low cost. In this study, gelatin microbubbles are synthesized with the help of Traut's reagent, and the relationship between their sizes and stabilities and experimental parameters such as solution pH, sonication time and amplitude, gelatin concentration to Traut's reagent ratio is explored. The reactivity of microbubbles with gelatin shell is characterized by quartz crystal microbalance with dissipation (QCM-D).

1.2 Overview of microbubble applications

1.2.1 Ultrasound Contrast enhanced agents

Microbubbles have been widely used as ultrasound contrast enhanced agents[1]. When ultrasound pulses are applied at a frequency close to the natural resonance frequency, the microbubbles can increase and decrease in size, producing very strong echoes in the region[2]. As a result, microbubbles can enhance the contrast in ultrasonic imaging; and microbubbles under 5 micrometres in diameter seem to work the best. The shells of the microbubbles help them get into the immune system and the gas core increases the echogenicity. Different materials have been used as shells for this application, including albumin, lipid and galactose[3].

1.2.2 Drug and gene delivery

One major goal for drug and gene delivery is to increase the concentration of drugs in the area of the disease while reducing side effects; and microbubbles have the potential to achieve this goal by using ultrasound for targeted delivery. Microbubbles with drugs or genes can be injected intravenously; and ultrasonic irradiation can act as the destructive force to administer where the microbubbles release their load or drug[4]. Considering that ultrasound is already widely used in imaging and easy to inject into the body, this method is relatively safe and simple to use. Furthermore, active microbubble targeting drug delivery has been achieved by linking ligands like antibodies and peptides to the surface of microbubbles, so that they can bind to specific receptors for drug delivery or diagmosis[4].

1.2.3 Particle capture and flotation

Microbubbles produced by injecting air into mineral slurry have been used to improve the recovery of fine particles in the flotation process[5]. Air can be dissolved into the solution under pressure, and the microbubbles will come out of the mineral slurry with fine particles upon the release of the pressure (e.g. dissolved air flotation). Because microbubbles can nucleate on the surface of fine particles, no additional attachment steps are needed. Considering that smaller particles usually float better with smaller bubbles, different pressure can be used to control the size of microbubbles and to achieve maximum recovery of fine particles. Other approaches to the generation of microbubbles on the surface of mineral particles are through hydrodynamic cavitation and ultrasonication. These two approaches have been extensively studied for fine particle flotation.

1.3 Challenges of microbubbles and objectives of this research

Although there has been a lot of research on microbubbles and their applications, many challenges still remain, especially for their applications in the most promising area: drug delivery. Throughout almost three decades of research, most of them were focusing on albumin as the shell for microbubbles. While albumin is a very suitable candidate, the limitation is the range of drugs that can bind to it. Meanwhile, gelatin has been used in pharmaceuticals for decades and food products for centuries[6]; therefore, it's very safe and benign for medical applications as compared to many other materials. As a denatured protein, gelatin has a low antigenicity[7], and has very accessible functional groups that can be used for further modification to target species. Gelatin nanoparticles have been used to deliver various types of drugs

successfully, indicating its potential for drug delivery[8], although their stability and mechanical properties still need to be improved. Glutaraldehyde has been used as a crosslinker to increase the stability of gelatin based micro- or nano-carriers, but its high toxicity presents a major concern for biomedical applications.

While gelatin shelled microbubbles have a promising future in drug delivery, however, a new method to crosslink gelatin without the use of glutaraldehyde is needed. Suslick et al. discovered the crosslinking process that involves the formation of S-S bond[9]; and Traut's reagent is the perfect agent to introduce thiol groups onto the gelatin surface to form S-S bond under ultrasound. Microbubbles prepared with gelatin and Traut's reagent can overcome most of the challenges mentioned above, making the stable gelatin-shelled microbubbles a reality in drug delivery and ultrasonic diagnosis.

After the microbubbles are synthesized, the most important physical property is bubble size. Many different factors can have an impact on microbubble size. Considering that the microbubbles with a diameter from 0.5 to 7 μm are the most desirable, it's important to study the relations between experimental parameters such as pH and ultrasonication and bubble sizes. Those parameters in turn can be used to control the generation of microbubbles of a desired size for applications. Furthermore, a two-step approach to make microbubbles was explored; and it has shown the potential to make protein-shelled microbubbles that are more suitable for the drug delivery application. Therefore, the objectives of this study can be summarized as below:

1. To synthesize gelatin-shelled microbubbles with the use of Traut's reagent.

2. To study the impact of different experimental parameters on the size of microbubbles, including gelatin concentration, pH, the ratio of Traut's reagent to gelatin, sonication time and amplitude.

3. To characterize the gelatin-shelled microbubbles using FTIR and SEM.

4. To study the surface reactivities of gelatin-shelled microbubble using QCM-D.

1.4 Thesis outline

This thesis is divided into 8 chapters. The first chapter is aimed to provide very basic background information and the formation of ideas presented in this thesis. The second chapter is the literature review that covered all three major elements of this research, i.e., microbubbles, gelatin, and Traut's reagent as well as how they are combined together to synthesize the gelatin-shelled microbubbles. The third chapter to the sixth chapter is the main part of this thesis, presenting the details of experiments and results. The third chapter mostly focuses on how the experiments are set up and why certain characterization techniques were chosen, including the fundamentals and working mechanisms. The fourth chapter is about the synthesis process of the microbubbles and some basic characterization including SEM and digital images, cross-section images, and QCM-D. The fifth chapter includes the effects various experimental parameters have on the size of microbubbles, and the discussion of possible ways to control the microbubble size and reactivity by adjusting those parameters. The sixth chapter is an extension of the synthesis process described in the fourth chapter, including a brief exploration of the two-step synthesis process and its great potential for future applications. The seventh chapter summarizes the major findings and conclusions of this thesis, with the eighth chapter of identifying areas that future

work may be conducted. The thesis is formatted in this way so that readers can read about this topic starting from an introduction and literature review, then gradually getting into experiment details and research outcomes, finally with a conclusion and brief summary for future research at the end. All references are attached after the main body of the thesis.

Chapter 2 Literature review

In this chapter, the literatures relevant to the research topic are reviewed and summarized. With the three major elements (microbubbles, gelatin, and Traut's reagent) of this research in mind, the chapter is organized as follows: Sections 2.1 to 2.4 are about microbubbles. In sections 2.1 and 2.2 the unique properties and advantages of microbubbles that led to this research are discussed; and then sections 2.3 and 2.4 focus on literature related to the synthesis of microbubbles. Section 2.5 discusses gelatin, and section 2.6 shows Traut's reagent. And finally, section 2.7 combines gelatin, Traut's reagents, and microbubbles to describe the synthesis of the gelatin-shelled microbubbles.

2.1 Unique properties of microbubbles

Microbubbles have shown many useful properties when combined with the use of ultrasound. They have great echogenicity, meaning that a backscattered echo can be produced at low acoustic pressures, which can in turn be used to detect the location of microbubbles. Therefore, microbubbles can be used as an imaging contrast agent. The echo is the strongest near their natural resonance frequency, which is directly related to the size of the microbubbles. A typical ultrasound imaging scanner operates at a range of 1-10 MHz, which is the resonance frequency of microbubbles with a diameter of a few micrometres. So microbubbles of this size range can produce the strongest signal and thus the most useful for ultrasound contrast imaging.

At higher acoustic pressures, microbubbles can become unstable and eventually fragment into smaller bubbles. The intense oscillation caused by higher acoustic power can cause the microbubble surface to go through cycles of compression and expansion, eventually causing the

bubbles to burst. This property can be very useful to eliminate microbubbles after their imaging or therapeutic usage.

At both high and low acoustic pressures, cavitation can happen when there is a long expansion phase followed by a compression phase in which the surrounding water squeezes the microbubbles so hard that results in the implosion of the microbubbles. The implosion can send a strong shockwave which can be detected. More importantly, the implosion can cause cavitation which may help with drug delivery.

Shells are often added to increase the stability of microbubbles; and most of the shell materials are from natural sources, like protein, lipids and other biocompatible polymers. Those shells can add additional useful properties to the microbubbles. They offer a good surface reactivity for further functionalization. And they can be treated or crosslinked with other biomolecules to add functional groups like anime, carboxyl or thiol on the bubble surface. Different shell structure and functionality can also offer different binding sites for various drug molecules. Typically, the shell materials are bio-friendly, and sometimes they can even carry certain ligands or be crosslinked with ligands that can bind with specific receptors. Through ligand-receptor interactions, targeted drug delivery can be achieved, which has great potential in therapeutic applications.

2.2 Advantages of microbubbles in various applications

Due to their unique property, microbubbles have many advantages when compared to other imaging or drug delivery methods. It's very cost-effective when compared to other molecular imaging methods like magnetic resonance imaging (MRI) or positron emission tomography

(PET)[10], and it's also very safe considering it's non-invasive without the use of radiation from computed tomography (CT) or PET[10]. As a drug delivery agent, shelled microbubbles are very bio-recognizable since most of the shell materials are natural proteins or lipids; and different ligands can be easily linked to the shells to target different species[11]. Furthermore, considering the drug release process is usually mediated by ultrasound, the cost-effectiveness and safety of ultrasound as previously mentioned are also very advantageous. By controlling the amplitude and frequency of the ultrasound, drugs can be only released in certain areas, increasing the concentration of drugs in desirable areas while reducing side effects. Procedures involving microbubbles are usually non-invasive as well[10], which can offer patients better comfort when compared to other therapeutic methods like chemotherapy. Overall, the unique properties of microbubbles give them many advantages over other approaches.

2.2.1 Microbubbles used in ultrasonic imaging

In the late 1960s, it was discovered that the oscillation of microbubbles can provide a strong contrast effect for ultrasonic imaging, and this can potentially be used clinically. However, this requires the microbubbles to be both small and yet stable enough to survive the internal environment and pass through the pulmonary capillary. In the 1980s, microbubbles that fit these criteria were first synthesized, and it came into commercial use in the 1990s. Microbubbles are advantageous when compared to other shell-core microsphere systems because the gas core is more compressible; and as a result, microbubble can provide much bigger backscattered signals. Microbubbles are also safer than many other liquid and solid cored microspheres. When compared to other imaging methods like MRI, it's also much more cost-effective to use microbubbles.

2.2.2 Microbubbles used in drug delivery

Since their successful application as ultrasonic contrast agents, more studies have been conducted to use microbubbles for drug delivery[12,13]. There are some apparent advantages over conventional drug delivery methods. First of all, using ultrasound, we can control the specific location of the drug release. Only areas that are hit by ultrasound will see the release of the drugs and the remaining drug loaded microbubbles will continue circling through the body. This will significantly raise the drug concentration in the treated area while minimizing the drug concentration in normal tissues elsewhere in the body, therefore mitigating side effects. This also means that a lower dosage of medications is needed because the medications administered are being more efficiently utilized. Second of all, using microbubbles as a vehicle can protect medications that are prone to degradation and thus make them more effective. Many modern medications are proteins, peptides or nucleic acids, and they can be fairly expensive. Using microbubbles can reduce the dose needed and make unrealistic or unaffordable treatment plans more feasible and realistic. Third, when compared to many other micro or nano level drug delivery vehicles, microbubbles especially with air as their core have fewer toxicity concerns[14].

There are two main ways for microbubbles to deliver drugs[15]. The first way involves the use of ultrasound and the process is shown below in Fig 2.1. Under the mediation of ultrasound, the microbubbles can be destroyed or fragmented to release the drug molecules into the cells around them. With high acoustic power, the microbubbles are ruptured[16], depositing drug molecules into target tissue cells. Due to the hydrodynamic instability induced by large oscillations[15], the ultrasonic power can cause microbubble cavitation, which in turn can help facilitate the process of drug deposition. After the microbubbles are destroyed, small holes are found on the

membranes of cells[11] and it's especially beneficial for molecules like plasmid DNA to get into the cell. The second way is using microbubbles to directly deliver the drug molecules without the use of ultrasound Many drug molecules such as proteins and plasmids[17,18] can bind to the protein shells of microbubbles to get delivered directly into cells that have certain specific receptors on their surface.
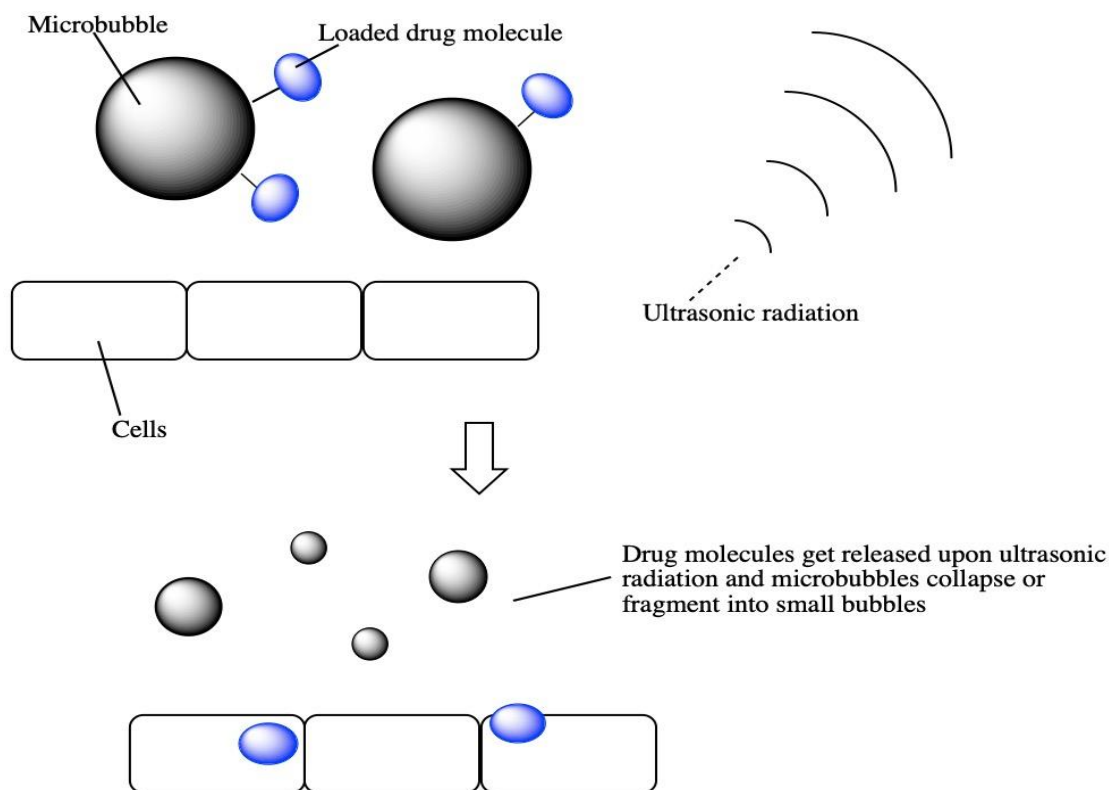
Figure 2.1 A schematic of drug-loaded MBs releasing drug molecules upon ultrasonic radiation.

2.2.3 Microbubbles used in particle capture and water treatment

Apart from their theranostic applications, microbubbles have also been used as agents to remove ions and particles from liquid solutions. Heavy metal ions can have severe negative impacts on the environment because of their toxicity and ability to accumulate along the food chain[19]. Many

treatment methods have been developed to eliminate or to reduce the concentration of metal ions in liquid solutions before they are released back to the local environment. When the particle concentration is high, solvent extraction is frequently used as a good and inexpensive way to treat the solution[20]; however, the long extraction time makes it inefficient for dilute solutions. Many new methods have been proposed and explored to improve the efficiency of the extraction process by increasing the interfacial area, one of which is using air microbubbles. Metals can react with proteins that contain cysteine[21]; so egg white protein (EWP) and bovine serum albumin (BSA) coated microbubbles were first used to remove metal ions from wastewater successfully[19]. It's also been observed that pH and temperature can affect the speed of absorption[22]; typically, higher temperatures will result in faster absorption and the optimal pH range is dependent on the specific metal ion.

Additionally, microbubbles can also be used to break down organic waste or microorganisms in wastewater[23]. Much like their application in ultrasound imaging, a large number of free radicals can be generated when microbubbles collapse, which can help decompose organic compounds to purify water.

2.3 Ultrasonic synthesis of microbubbles

2.3.1 Synthesis procedures

Proteinaceous microbubbles with bovine serum albumin (BSA), human serum albumin (HSA) and lysozyme as their shell have been successfully synthesized by previous researchers using ultrasonic irradiation[24]. Typically, a 2%- 5% w/v protein solution was prepared, and an ultrasonic horn was placed at the water-air surface, then the solution was sonicated for a certain amount of

time ranging from 15 seconds to 3 minutes. The temperature and pH of the solution, as well as the time and amplitude of the sonication process, can affect the yield and size distribution of microbubbles. After the synthesis, filtration or centrifugation was sometimes used to separate or concentrate microbubbles of a certain size.

2.3.2 Mechanism

The ultrasonic irradiation process can produce emulsification and cavitation, and both of them are important in the microbubble synthesis process. The emulsification process helps air to be dispersed into the aqueous solution; and it's the foundation of the synthesis of microbubbles. However, emulsification itself is not enough to produce stable and long-living microbubbles. The cavitation process in which tiny air bubbles form, grow and collapse can generate high energy, and as a result a lot of free radicals will be produced, for example OH· and H·. Those free radicals will then form superoxide and peroxide, both of which can act as cross-linking agents for protein.

The presence of superoxide and peroxide is very essential, as is Cysteine which can be easily oxidized by those agents; and this is proved by further experiments carried out with various inhibiting chemicals to prevent oxidation[25]. As is shown in Fig 2.2 below, when superoxide dismutase is added, the yield of microbubbles dropped significantly; and when N-ethylmaleimide and glutathione were added, the synthesis of microbubbles was completely stopped. This showed that the presence of superoxide is vital to the synthesis process.
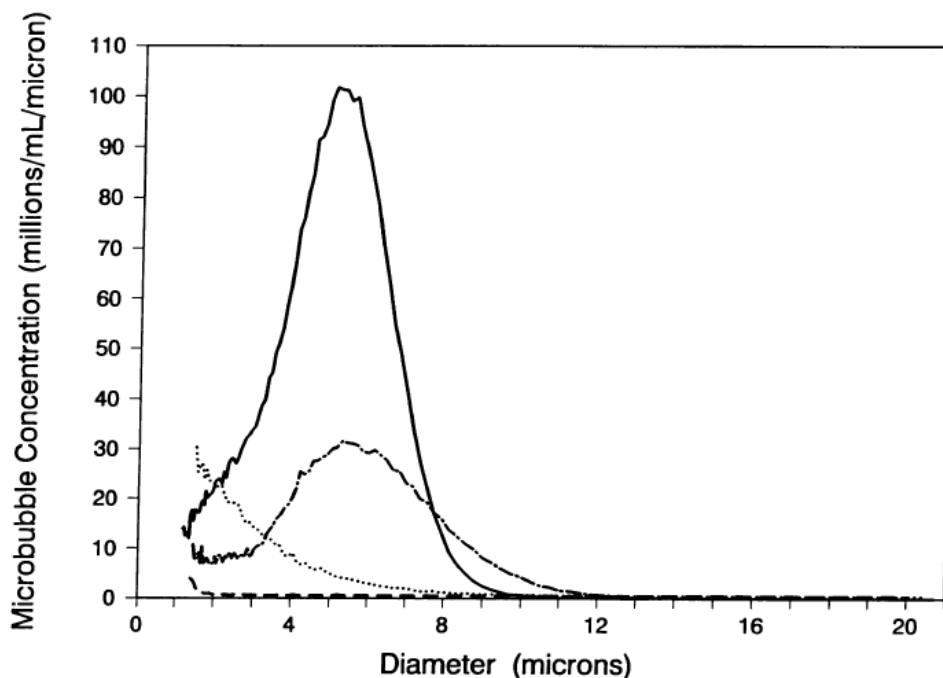
Figure 2.2 Synthesis of microbubbles with different chemicals to prevent oxidation[25]. —, 5% w/v BSA; —·—·, 5% w/v BSA and 0.2% superoxide dismutase; ····, 5% w/v BSA and 0.04% M N-ethylmaleimide; - - - -, 5% BSA w/v and 0.2% 0.1M glutathione.

Furthermore, experiments with Myoglobin (Mb) that don't have Cysteine residues showed microbubbles cannot be formed[26]. When cysteine residues reacted with N-ethylmaleimide to prevent oxidation, the yield of microbubbles went down significantly[25,27]. Thus, it's concluded that the presence of Cysteine residue and the formation of disulfide bonds were important to synthesize microbubbles.

Many efforts were made to increase the presence of Cysteine residues, or thiol groups. Two major approaches were explored, heat denaturation and chemical denaturation. Heat denaturation

aimed to loosen the protein structure in an attempt to break internal disulfide bonds to expose them to the superoxide during the synthesis process[28]; however, it's not very effective considering that the disulfide bond is relatively insensitive to high temperatures. Chemical denaturation involves the use of reductants, which can reduce the internal disulfide bonds to free thiol groups[29-31]. This approach has been successful[29] and a higher degree of denaturation usually resulted in a higher degree of cross-linking. However, it heavily depends on proteins that have ample amounts of disulfide bonds; otherwise, there won't be any thiol group even after the denaturation, and therefore the synthesis of microbubbles won't be possible.

2.4 Shelled microbubbles

2.4.1 Mechanism

For an air-bubble suspended in water, according to the Young-Laplace equation,

$$\Delta p = \frac{2\gamma}{R}$$
(Eq. 1)

In which Δp is the pressure difference between inside and outside of the bubble, γ is the surface tension and R is the radius of the bubble, assuming the bubble is of a spherical shape. For larger bubbles, for example when R > 100 μm, the pressure difference is relatively small when compared to air pressure; but for smaller bubbles, the internal pressure may rise significantly. As a result, air will dissolve into the surrounding unsaturated solution, causing the bubbles to shrink and disappear. Theranostic applications require microbubbles to be around 1 to 10 μm, but small microbubbles without any encapsulation are very unstable and have very limited lifetime[16]; so additional measures to stabilize microbubbles are needed. One theory is to use a hydrophobic gas

to form bubbles, it can saturate the surrounding solutions much faster to increase the lifetime of the bubbles[32], but the use of hydrophobic gas can severely limit the applications of microbubbles; and even gases like perfluorobutane can't make the microbubbles stay for longer than a minute[11]. So a better way to stabilize the bubbles is needed. Coating microbubbles with other materials, such as proteins or lipids, can lower the surface tension or even effectively eliminate the surface tension[16] (γ is possibly close to 0). Surface tension on the interface stems from asymmetrical forces experienced by the surface water molecules; the added shell material can interact with those water molecules and thus lower the surface tension. This can increase the lifespan of microbubbles exponentially.

2.4.2 Materials

The basic structure of a shelled microbubble is shown below in Fig 2.3. The gas core is enclosed within the rigid shell; and different types of shells have been explored, including protein, lipid, polymer and surfactant[33]. The selection of shell materials is usually based on the intended function of the microbubbles, mostly ultrasonic imaging and drug delivery.
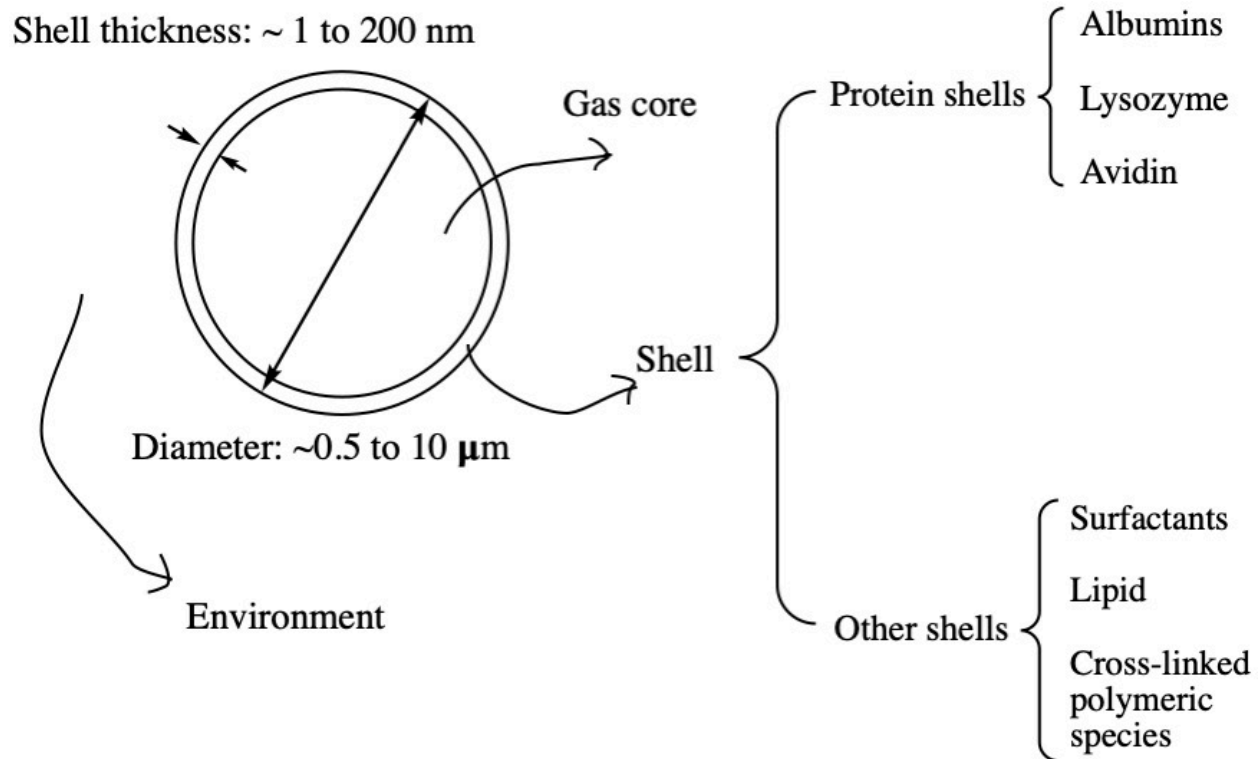
Figure 2.3 Polymeric core-shell microbubbles.

a) Protein shells

Albumin is the most commonly used protein for microbubble shells, both human serum albumin (HSA) and bovine serum albumin (BSA) have been intensively studied[25,34,35]. Albunex, a microbubble solution with HSA as the shell, became the first commercially approved and certified echocardiographic contrast agent[36]. Albumin is very desirable as shells because it's relatively cheap, has low toxicity, soluble in water, and more importantly, it has the ability to cross-link with each other through covalent bonds. There are many cysteine residues in albumins and they can form disulfide bonds upon sonication as explained in section 2.3 therefore making

the shell more stable and rigid. BSA microbubbles were also synthesized using different

methods, and the stability of microbubbles is improved[37-39]. Although there are reports that

cysteine residues are not necessarily needed for proteins to act as shells for microbubbles[40], the

synthesis process can be a lot harder and more unpredictable without them. Other proteins that

have been used include lysozyme[29,41], which also confirmed the importance of disulfide bonds.

Additionally, Korpanty et al. incorporated avidin into the protein shell along with albumin[42], and

used it as an anchor to link with antibodies to use in vascular targeting and molecular imaging.

b) Other types of shells

Surfactants, lipid and cross-linked polymeric species were all used as shells of microbubbles.

Synthetic surfactants SPAN-40 and TWEEN-40 have been used to form stabilized microbubbles

by Wheatley et al[43,44]. They were generated using the sonication method with the presence of air.

Lipid shells were first introduced to emulate the stability of pulmonary surfactant[45]. The major

advantage of lipid shells is that they have hydrophobic and hydrophilic groups, so they can form

a highly oriented layer around the water-air interface, and when the water-air surface gets

sonicated, the lipid layer will spontaneously entrap the gas bubbles and become the shell, with

the hydrophobic end facing the gas core and hydrophilic end facing the water. Other types of

mixed or multi-layered shells were also being used, they are typically thicker so they can make

the microbubbles more resistant to the environment, but at the same time reduce the echogenicity

of the microbubbles. Depending on the specific material, many mixed or multi-layered shells

don't have a good ability for drug delivery when compared with protein and lipid shelled

bubbles. Examples for these microbubbles include the double-ester polymer encapsulated

microbubbles made by Bjerknes et al[46] and PLGA (poly(D,L-lactide-co-glycolide)) microbubbles made by Nayaran and Wheatley[47].

2.5 Overview of gelatin

Gelatin contains a mixture of peptides and proteins. It is extracted from the tissues, skin and bones of animals. Throughout the years, people have found many uses of gelatin, and the first usage can be traced back to the 1400s in the Middle East[48]. Historically, it has been used for food for many centuries, being made into jelly or gelatin powder, as well as acting as a gelling agent in cooking. More recently, gelatin has been widely used in various industries. Most of the shells of drug capsules are made from gelatin to help patients swallow them; many cosmetic products contain gelatin; it can be found in paintballs as well to make their shell; some vaccines such as MMR (measles, mumps, and rubella) have gelatin to shield the viruses from heat or freeze-drying, so that they can stay effective even after exposure to extreme conditions; even clothes can be made out of gelatin. Its low cost and easy fabrication process have led to its wide application in our life.

Gelatin is most commonly sourced from pigs and cows, but can also come from chicken, fish or other animals. Pig skin is the most common source of gelatin, accounting for 44% of the overall production, while bovine skin accounts for another 28% and bones for 27%. The most common amino acid in gelatin is glycine, followed by hydroxyproline and proline, as shown in Figure 2.4.
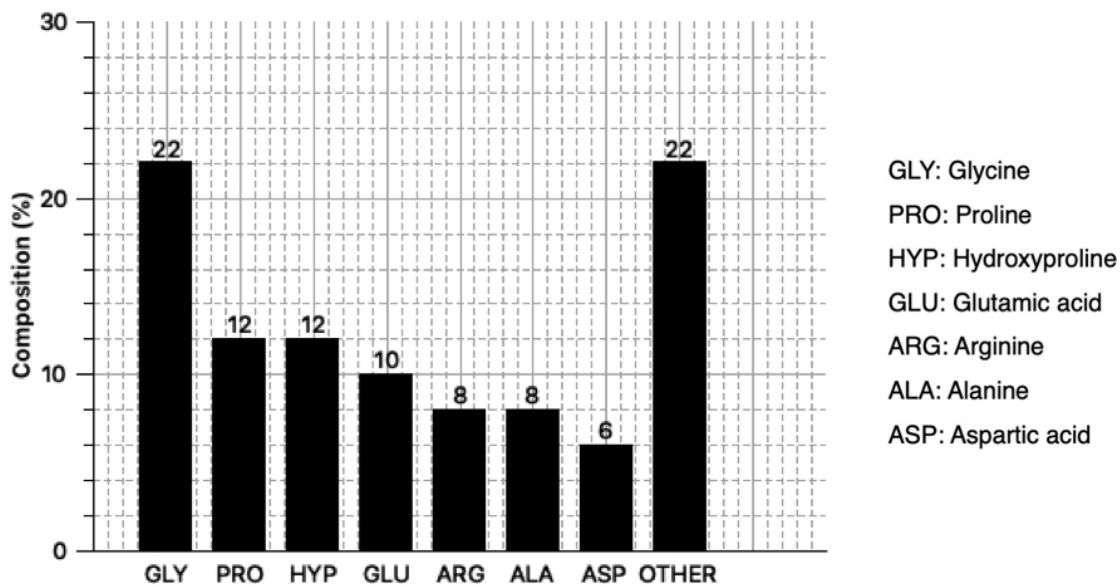
Figure 2.4. Amino acid composition of gelatin.

Gelatin can stimulate skin collagen production; researchers have found that gelatin ingestion can largely increase the size and density of collagen fibrils and fibroblasts[49]. Gelatin is also found to have a positive effect on joint pain, especially with the most severe cases. Nomura, et al. found that oral intake of shark gelatin can lead to an increase in bone material density in rats[50].

Gelatin is also widely used to coat cell culture plates; it can help many different cell types to attach to the plate. Research has shown that gelatin can be used as a blocking agent for non-specific binding during the enzyme-linked immunosorbent assays (ELISAs) process. During the bacteria culturing process, gelatin can be used in the media to help with species differentiation[51].

As a natural polymer, gelatin has great biocompatibility; so it's used in many pharmaceutical and medical applications. One of them is as a protein drug carrier. Because gelatin can be made from two different (acid and alkaline) processes, its electrical properties can be modified during the fabrication process, resulting in gelatin with different isoelectric points. Thus, an oppositely charged gelatin molecule can be used to interact with the protein drug to form a polyion complex. The polyion complex can be degraded by enzymes over time in the body, and the degradation speed can be controlled through the extent of crosslinking. Eventually, the protein drugs will be released from the complex. Considering that the polyion complex system is very common in the body's natural biological process, the gelatin protein drug system can be very effective for the sustained release of the drug. Furthermore, theoretically gelatin can form polyion complexes with any positively or negatively charged biomacromolecules tod release them into the body through the degradation of the crosslinking.

Another important biomedical application of gelatin is tissue engineering[52]. Because of its biocompatibility and biodegradability, gelatin is a very desirable material for tissue engineering. In cardiac tissue engineering, research has shown that gelatin can be used to form a scaffold for cells from fetal rat ventricular muscle to grow, in both in vitro and in vivo environments[50]. Other studies have demonstrated that when combined with other materials, gelatin scaffolds can have different degradation rates; and the scaffolds can be specifically fabricated to simulate natural cardiac tissues[50,51,53-56].

2.6 Traut's reagent

Traut's reagent (2-Iminothiolane) was synthesized by R. R. Traut and his team in the 1970s[57,58]. Traut's reagent primarily reacts with primary amines (-NH$_2$) and it can introduce sulfhydryl (-SH) groups onto the protein. When compared with other reagents that can be used for this purpose, Traut's reagent itself contains no sulfhydryl group, so it's more stable as it can resist oxidation better[58]. Since its first synthesis in the 1970s, Traut's reagent has been widely used in many protein modifications to help with cross-linking or to study protein's structures. As it's mentioned before, -SH functional group is a key to successful crosslinking to form a stable shell for microbubbles. So Traut's reagent can serve as the perfect reagent to introduce -SH group to proteins that don't have natural -SH residues.

2.7 Gelatin shelled microbubbles

Gelatin is a very promising proteinaceous material to be used as a shell for microbubbles. It has several advantages over other potential materials. First, it is a natural polymer, non-toxic so it presents a low risk for biomedical applications[59]. Second, it has low antigenicity. Third, gelatin has many functional groups that can be easily modified and used as binding sites. Last, gelatin is relatively cheap and also has been extensively studied as discussed in section 2.5 so many of its properties are already known.

Because of the aforementioned favourable characteristics of gelatin, researchers have been working on a gelatin-based protein microbubble system for a long time; but unlike HSA or BSA shelled microbubbles which already had commercial success, it's difficult to get stable yet small gelatin-shelled microbubbles. Initially, gelatin without any crosslinking was used, and stable

microbubbles couldn't be formed. So crosslinking was the next natural step; aldehydes are a very popular group of protein crosslinking agents; so glutaraldehyde was first used on BSA microbubbles[60], and then on gelatin microbubbles as well[61].

Tabata and Ikada synthesized and studied gelatin microbubbles in the 1980s[61] for drug delivery purposes. They used glutaraldehyde to cross-link gelatin and subsequently, multiple studies were conducted to investigate the process of cross-linking gelatin with glutaraldehyde and the benefits and drawbacks of this procedure[62]. Glutaraldehyde can react with protein at room temperature. The reaction is very fast and also very easy to observe. However, due to the toxicity of glutaraldehyde, there are great concerns with glutaraldehyde as the crosslinking agent, especially when used in drug delivery.

To summarize, protein shelled microbubbles have great potential in many applications and gelatin has many advantages if it can be used as the shell. However, due to the lack of natural cysteine, stable gelatin microbubbles can't be synthesized using the sonication method that was used to synthesize BSA/HSA shelled microbubbles. Glutaraldehyde was initially used as a cross-linking agent with success, but its toxicity greatly limited the potential applications. A new way to modify gelatin is needed. As detailed in section 2.6, Traut's reagent can serve as the perfect agent to add -SH groups onto gelatin, and make the synthesis of gelatin microbubbles possible. This new approach will also pave the road for other proteins that lack natural cysteine but are otherwise suitable to be used as microbubble shells.

Chapter 3 Experimental setups and materials

3.1 Field Emission Scanning Electron Microscopy (FE-SEM)

Optical Microscopes can usually only go up to 1,000x, so it can be very difficult to see the microbubbles, and almost impossible to observe its surface morphology. It can also be very challenging to differentiate microbubbles and protein aggregates. In comparison, SEM can provide a lot more information that conventional optical microscopes can't, from surface topology, chemical composition to electrical behaviour of the surface layer of samples[63]. SEM uses electrons that are accelerated to high energies, and usually uses the secondary electrons that are reflected off specimens to create an image[64]. There are different electron guns that can be used for SEM, specifically for FE-SEM, which uses a field emission gun to provide a very bright beam with very little electron energy variation[65]. After the secondary electrons are accelerated, they strike the scintillator and emit light. Then the photomultiplier changes the light signal to an electrical signal and amplifies it, allowing the software to produce a digital image. An in-lens secondary electron (SE) detector was used to get all the images in this thesis, because when compared to conventional SE detectors, in-lens detectors can collect secondary electrons with higher efficiency, allowing users to get good images at lower voltages and smaller working distance. This is favourable because higher voltages can potentially damage or burn the fragile samples. Fig 3.1 below is a schematic diagram drawn to show the structure of the SEM used in the experiments (Zeiss Sigma FE-SEM). The field emission gun is at the top, producing a laser beam that gets accelerated in the beam booster. The beam hits the sample, then the secondary electrons that are reflected from the sample are collected by the detector in the middle.
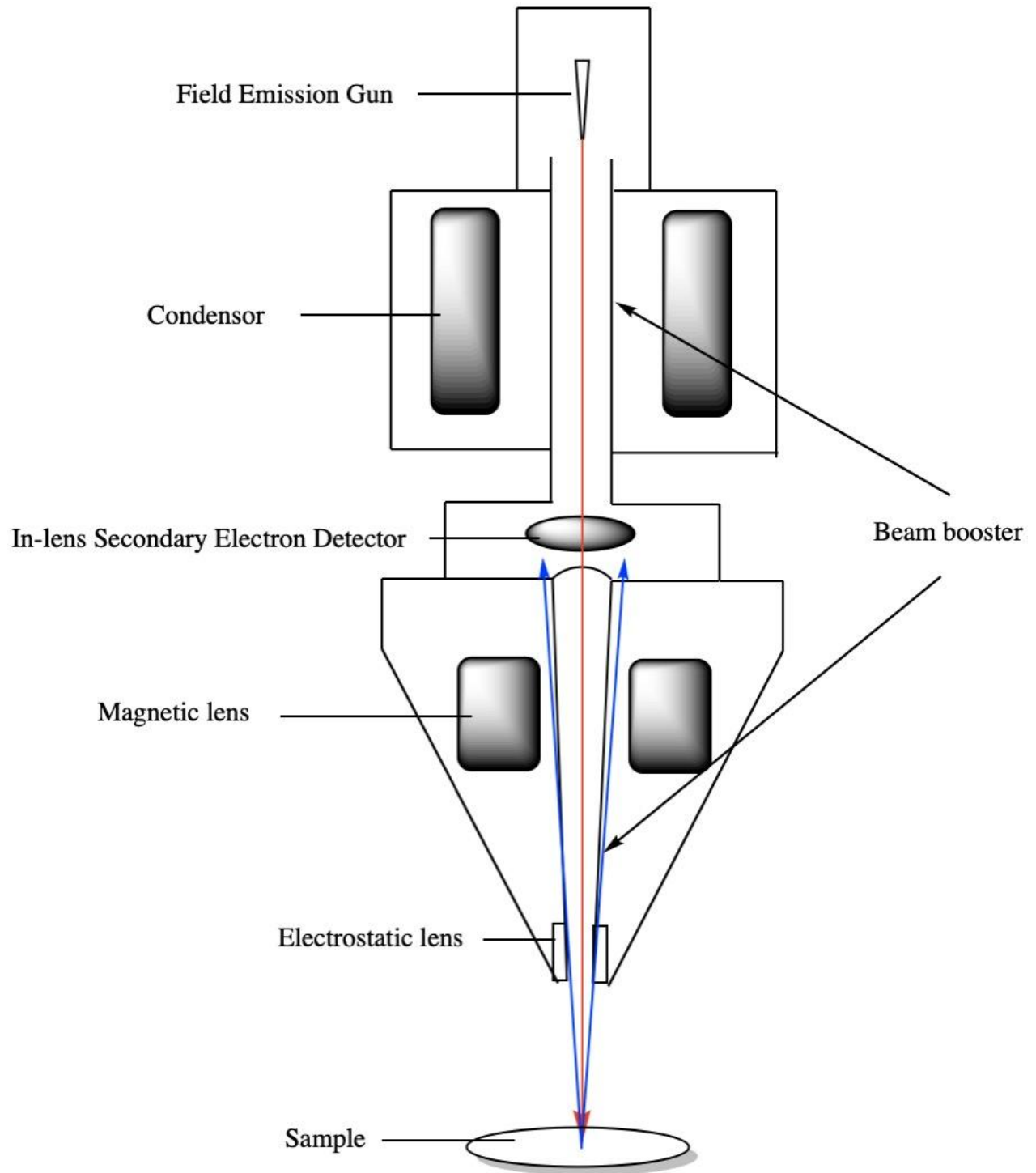
Field Emission Gun

Condensor

In-lens Secondary Electron Detector

Magnetic lens

Electrostatic lens

Sample

Beam booster

Figure 3.1 A schematic diagram of FE-SEM.

3.2 Carbon coating and SEM sample preparation

To prepare for FE-SEM imaging, all samples have to be completely dry and electrically conductive. So a small aliquot of Gel-MB (gelatin microbubbles) solution was carefully dropped onto a silicon wafer, and left at room temperature for 24 hours until it's completely dry. Then the wafer was broken into small pieces similar to the size of an SEM stub and taped onto stubs with carbon tapes. A thin layer of carbon was sputtered onto all samples to increase its conductivity. Carbon coating was chosen over gold coating because of the smaller particle size and more precise control of coating thickness. Leica ACE600 carbon coater was used in single pulse mode, and all samples were coated with 5 nm of carbon.

3.3 Spectrophotometry

A spectrophotometer can measure the intensity of light at a selected wavelength, and by comparing the absorption difference of blank solutions and sample solutions, it can be used in a wide range of quantitative analysis[66]. There are two main parts, a spectrometer and a photometer[67]. The spectrometer produces light at a given wavelength, and after the light goes through the sample, the photometer then collects the signal and then translates it to a digital signal. By comparing the intensity of the light that passes through the sample (I_t) and the intensity of the original light beam (I_0), absorbance (A) can be calculated as follows:

$$A = -\log (I_t/I_0) \tag{Eq.2}$$

According to Beer-Lambert law,

$$A = \varepsilon l c \tag{Eq. 3}$$

Where ε is the absorption coefficient, l is the path length, and c is the concentration. So with any given wavelength and specific substance, ε is a constant, l is the cuvette width which is usually 1 cm, c can be calculated with the measured absorbance. Different molecules and compounds absorb or transmit light over a certain wavelength differently, so by measuring the absorbance of light at a certain wavelength, the concentration of a given compound can be calculated; and it's a very useful method to prove the existence of a chemical or to estimate its concentration. In the experiments, it's used to prove the presence of thiol groups.

3.4 FTIR

FTIR (Fourier Transform Infrared Spectrometer) has been widely used in chemical synthesis and analysis. FTIR utilizes infrared light to determine the structures of chemicals by detecting the molecules' absorption of infrared light. Molecules that contain certain bonds can selectively absorb radiation of specific wavelengths, while allowing others to pass through. The signals are then detected, and a spectrum of radiation absorption is plotted, from which chemical structures of the sample molecules can be determined.

Figure 3.2 below showed the components of an FTIR spectrometer. The source emits infrared radiation, then the beam splitter transmits and reflects 50% of the radiation. One beam reflects off a fixed mirror, the other one reflects off a moving mirror. The two beams are then recombined to go through the sample and then reaches the detector. As the moving mirror's position changes, the resulting signal also changes which gives information about absorption at every infrared frequency coming from the source.
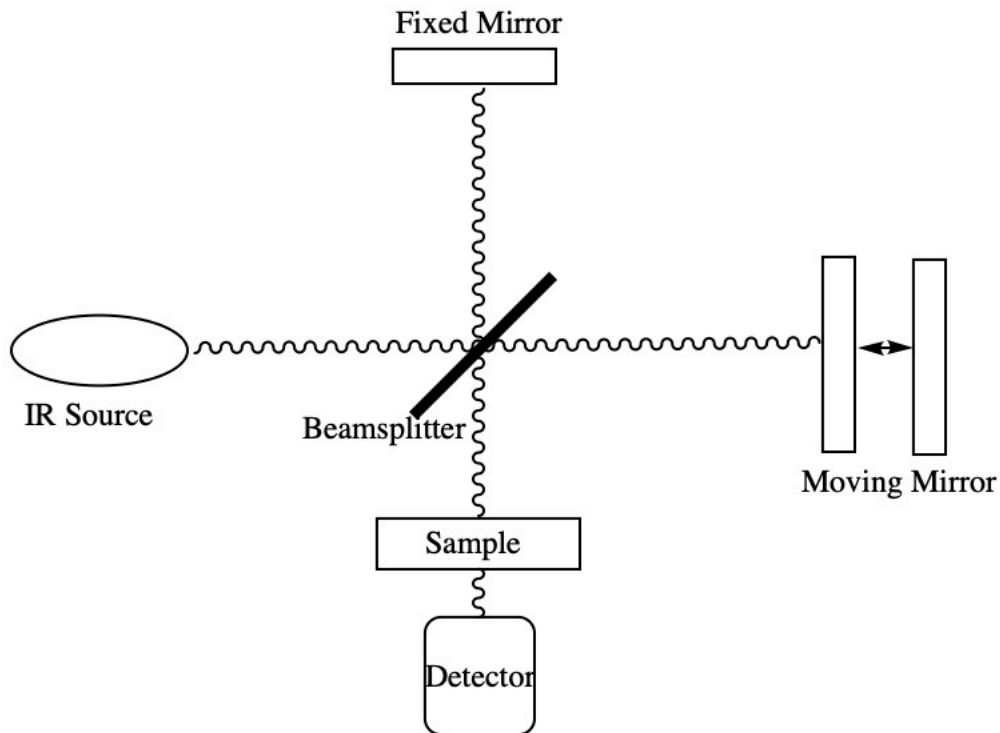
Figure 3.2 Components of an FTIR spectrometer.

3.5 Dynamic light scattering

Dynamic light scattering (DLS) is the most commonly used technique to determine the size

distribution of small particles. DLS measures the Brownian motion of particles and then uses the

Stokes-Einstein equation to calculate the hydrodynamic diameter of particles. Brownian motion

is the random movement of particles suspended in a solution due to their collision with

surrounding solvent molecules. Energy transfer happens with every collision and the energy

transferred remains more or less constant; so smaller particles will have a faster speed as a result.

So we can determine the hydrodynamic size of the particles if we can measure their speed, and

their relations are given by the Stokes-Einstein equation:

$$R_H = \frac{k_B T}{6\pi\eta D}$$
<div align="right">(Eq. 4)</div>

Where R_H is the hydrodynamic radius, D is the translational diffusion coefficient, k_B is the Boltzmann's constant, T is temperature and η is viscosity. R_H is the size of a sphere that has the same diffusion rate and hydrodynamic behaviours as the particles being measured, so the further a particle is from a perfect sphere, the further the R_H is from its effective radius. In the experiments, most microbubbles are very close to spheres in shape, and their applications are mostly related to their hydrodynamic properties; so R_H is the radius most often used and measured by researchers.

To get D, a typical DLS setup will use a laser to shine through the solution and measure the fluctuation of scattered light intensity over time. The auto-correlator is used to compare the similarity of two signals separated by a small time interval. When the time interval is relatively long the signals won't be closely correlated because of the randomness of Brownian motion; but if the time interval is very small, they will be strongly correlated. For smaller particles, the degree of correlation will decrease much faster than that of bigger particles, so the auto-correlator can use the point starting at a significant decay in correlation to determine the particle size.

Specifically, a Malvern zetasizer nano was used in the experiments, with a detection angle of 90 degrees and a laser wavelength of 633 nm. Since it's very difficult to determine the exact values of refractive index and absorption of gelatin-shelled microbubbles based on literature values, size distributions by intensity were used throughout the measurements instead of volume or number distributions.

3.6 QCM-D

Quartz Crystal Microbalance (QCM) is a highly sensitive device that can measure weight changes up to the nanogram in scale. Quartz, as a piezoelectric material, can oscillate at a certain frequency when an alternating voltage is applied to it by electrodes. When the mass of the sensor with its surface layer changes, so does the oscillation frequency; therefore, QCM can operate as a very sensitive microbalance by simply measuring the change of the resonance frequency. It is very useful in obtaining information about reactions and interactions that happen at the sensor surface.

The Sauerbrey equation describes the relations between oscillation frequency change (Δf) and mass change (Δm):

$$\Delta m = -\frac{C\Delta f}{n} \qquad\qquad\qquad\qquad\qquad\qquad\qquad\qquad \text{(Eq. 5)}$$

Where C is a constant depending on the property of the material and n is the overtone number. Typically for a 5MHz quartz crystal, C=17.7 ng/(Hz· cm^2). So tiny mass changes can be calculated from the measured frequency changes. However, one condition for Sauerbrey's equation is that the added mass should be attached to the surface rigidly, so this equation alone can't accurately describe the relationship between frequency and mass when it comes to viscoelastic samples. Those samples can interact with the crystal surface and form a layer of viscoelastic film; and the film can cause dissipation of oscillation energy, so that dissipation needs to be taken into account to accurately measure the mass.

QCM-D can measure the energy loss (dissipation) in addition to the frequency change of the freely oscillating sensor. The voltage applied to the sensor is turned off after exciting it to its resonance frequency, and then the time it takes the oscillation to stop is measured. When molecular adsorption happens at the surface, the molecular layer will increase the dissipation while decreasing the frequency. Because the entire process happens at the millisecond scale, real-time data can be obtained about the adsorption process; so it's faster and more accurate than usual QCM measurements, and it's extremely helpful for studying the interactions of biomaterials and different surfaces [68].

3.7 Experimental materials

3.7.1 Chemicals and other consumables

Gelatin (porcine, type A, bloom number 90 -110), Traut's reagent (2-Iminothiolane), Phosphate-buffered saline (PBS) solution, 1-ethyl-3-(3-dimethylaminopropyl) carbodiimide (EDC) and ethylenediamine were purchased from Sigma-Aldrich, Ellman's reagent (5,5'-dithiobis-(2-nitrobenzoic acid)) was purchased from Thermo Fisher Scientific. Zeba spin desalting columns (7 K, 2 ml, 5 ml, 10 ml) and centrifuge tubes (15 ml, 50 ml) were also purchased from Thermo Fisher Scientific.

3.7.2 Equipment

A Fisher Brand dismembrator model 705 with a micro-tip (3 mm in diameter) was used as the ultrasonic source. An Innova 42 incubator shaker series was used to incubate solutions. A Labconco freezone 4.5 was used to freeze dry samples. A Fisher Scientific XL 20 pH meter was used to measure pH. An Ohaus AX224/E balance was used to measure the weight of chemicals.

A Q-Sense QCM-D and an ISMATEC high precision multichannel dispenser were used for QCM-D measurements. Silica, alumina and gold sensors were purchased from Q-sense. A Malvern Zetasizer Nano-ZS was used for size distribution measurements. A Zeiss-Sigma Field Emission SEM was used for SEM imaging. A Leica ACE600 carbon/metal coater was used to coat the samples for SEM imaging. A Keyence VHX-700F digital microscope was used to obtain digital images. A Shimadzu UV-3600 was used for absorption measurements. A Thermo Fisher Nicolet iS50 FT-IR was used to obtain FTIR spectra.

Chapter 4 Synthesis of gelatin-shelled microbubbles

4.1 Synthesis process with Traut's reagent

4.1.1 Preparation of the buffer solution

Various buffers can be used for the thiolation process with Traut's reagent. The most common one is PBS with its pH adjusted to 8[57,58]. 5 mM EDTA is used to prevent the oxidation of free thiol groups. The buffer solution was made in 100 ml batches for consistency throughout experiments, and pH measurements were performed every time before new microbubble synthesis to ensure the quality of the buffer solution.

4.1.2 Gelatin and Traut's reagent reaction

Type A gelatin with a gel strength of 90 -110 g bloom has an average molecular weight of about 23 kDa[69]. 250 mg of gelatin and 29.9 mg of Traut's reagent were mixed in 5 ml of buffer solutions to make a 5% w/v gelatin solution, and Traut's reagent is 20 times the molar concentration of gelatin. The effect of gelatin's concentration and the ratio of gelatin and Traut's reagent on microbubble properties are further discussed in Chapter 5.

Gelatin and Traut's reagent were incubated in an incubator (New Brunswick Innova 42/42R) at 45 °C with a gentle shake of 60 rpm for an hour. 45 °C temperature will help loosen up gelatin's structure, improve its solubility, and also speed up the reaction. After the reaction, the solution appears to be light yellow and transparent. Spin desalting columns were used to remove remaining Traut's reagent after the reaction[70]; in short, they were centrifuged at 1000 relative centrifugal force (RCF) for 2 minutes to remove the storage solution, then loaded with buffer and

centrifuged for 2 minutes, repeated for 2 more times, and finally loaded with gelatin-Traut's

reagent mixture and centrifuged at 1000 RCF for 2 minutes to remove most of unreacted Traut's

reagent[71].

4.1.3 Ultrasonication process to generate microbubbles

A fisher scientific 705 dismembrator was used to generate ultrasonic radiation of 20 kHz. A 3

mm diameter micro-tip was put onto the air-water interface[72], and the ultrasound was applied at

25% amplitude for 45 seconds for a total of 330 J. The amplitude and time of the sonication

process can have major impacts on the size of the microbubbles and their effects are further

discussed in Chapter 5. After the sonication, there was a lot of foam on top, containing large and

visible bubbles, and the aqueous phase was at the bottom, containing the microbubbles. Over

time, the big bubbles on top would burst, reducing the purity of the synthesized microbubbles at

the bottom; so it's important to withdraw the aqueous phase with a pipette as soon as the

sonication process was finished. The aqueous phase was then carefully put into a new tube and

stored at 4 °C. Fig 4.1 below showed the synthesis process, and the microbubbles have a shell-

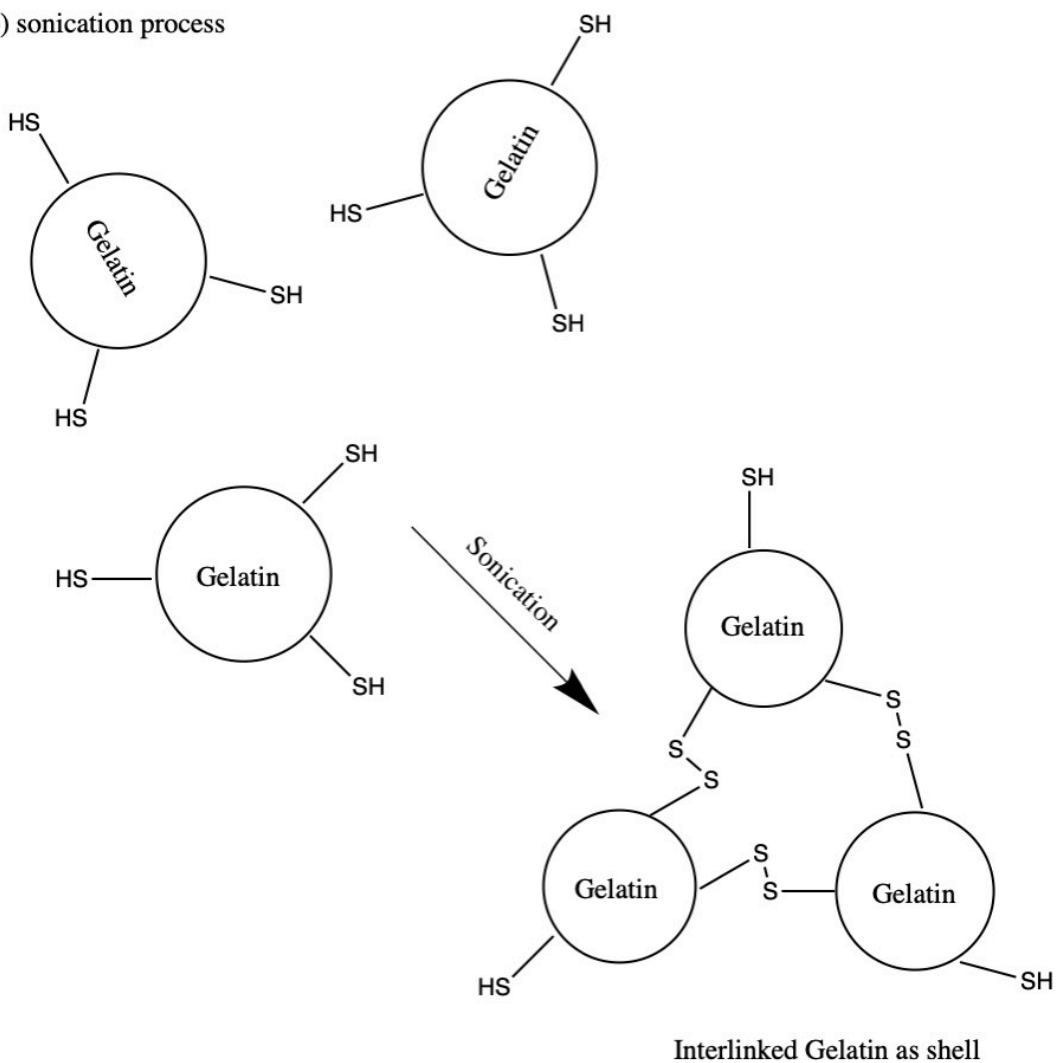core structure with air as the core and interlinked gelatin as the shell.
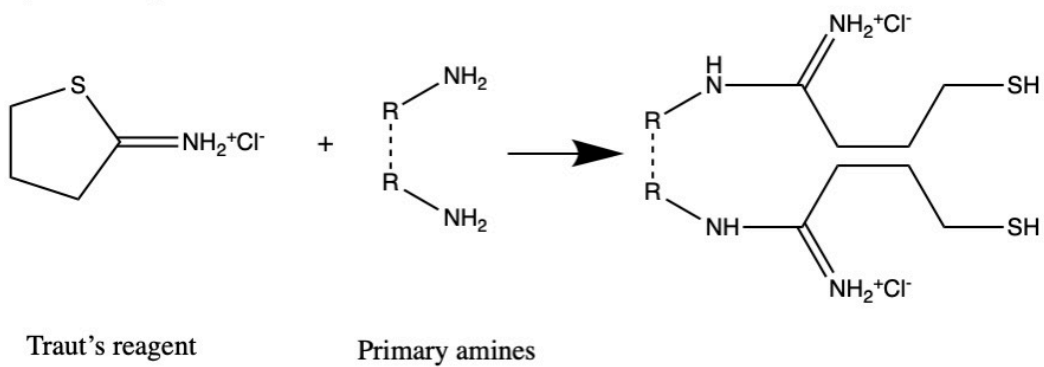
Figure 4.1 Microbubble synthesis process; a) thiolation process; b) sonication process.

4.2 Quantification of free thiol groups

To prove the successful thiolation of gelatin and subsequently the successful formation of the linked gelatin shell, two methods were considered. First is FTIR (Fourier-transform infrared spectroscopy), S-H bond has a weak peak at 2550 - 2600 cm^{-1}, and some previous researchers[70] were able to detect the peak in this region to prove the existence of free thiol groups; but in general the peak is very weak[73] and easy to overlook due to other surrounding peaks. FTIR was conducted with a Nicolet iS50 spectrometer with the ATR (attenuated total reflectance) module at wavenumber from 700 to 3700 cm^{-1}, and recorded spectra were shown below in Fig 4.2 and Fig 4.3. Fig 4.3 zoomed in from 2400 to 3000 cm^{-1}, and a small 'peak' or plateau area can be identified around 2640 cm^{-1}, possible evidence of the S-H bond. However, given the size of the peak and a slight shift from the peak's literature value, further experiments were needed to prove the successful thiolation process.
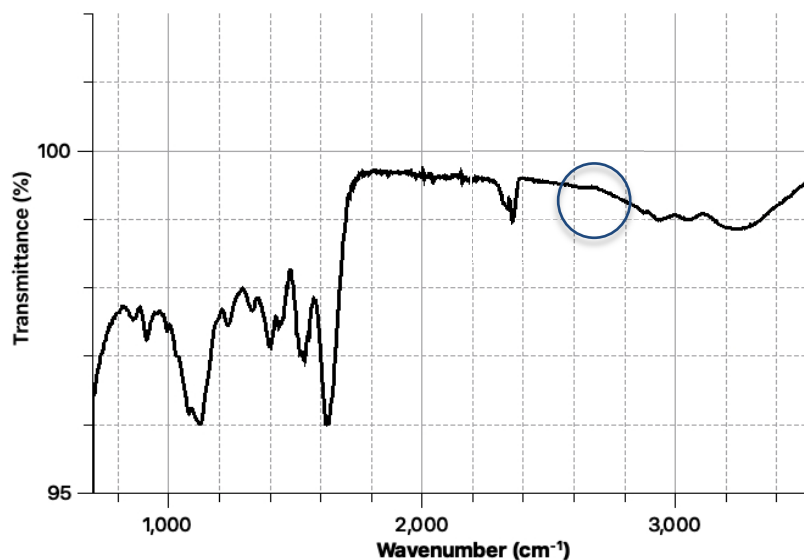

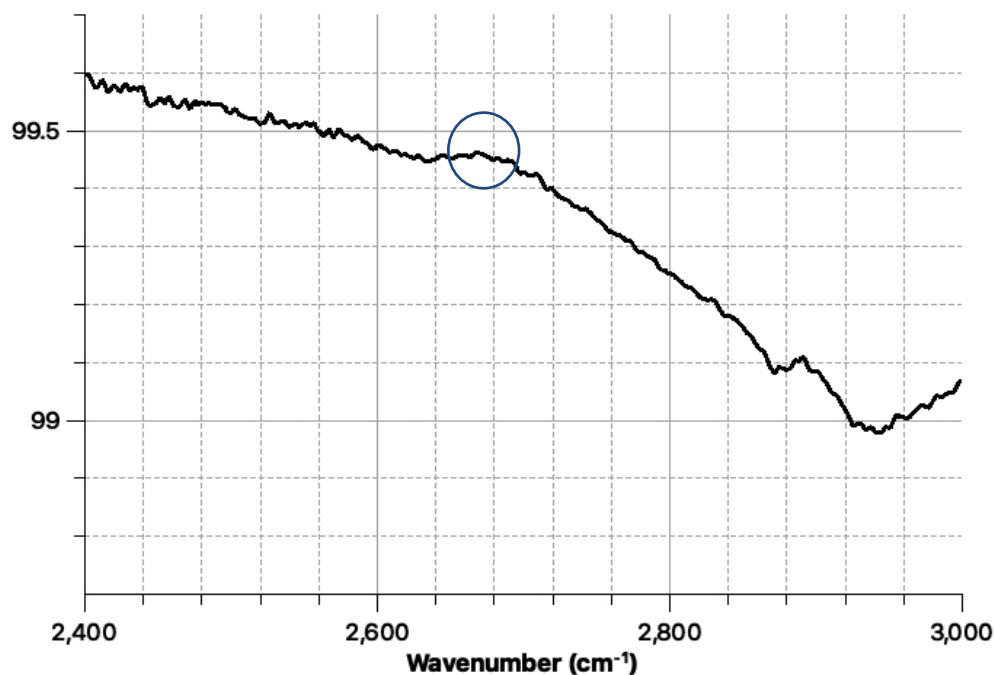Figure 4.2 FTIR spectrum of gelatin-shell microbubbles.

Figure 4.3 FTIR spectrum of gelatin-shell microbubbles from 2400 to 3000 cm^{-1}.

The second method was to use Ellman's reagent. In 1959 Ellman first introduced the use of 5,5'-dithio-bis-(2-nitrobenzoic acid) (DTNB) as an agent to quantify free thiol groups[74]. Ellman's reagent can react with free thiol groups and form TNB (5-thio-2-nitrobenzoate) anions, and TNB is coloured and has a molar extinction coefficient of 14,150 M^{-1} cm^{-1} at 412 nm. By measuring the absorbance of TNB at 412 nm the concentration of thiol groups in the original solution can be estimated. The reaction mechanism is shown below in Fig 4.4.
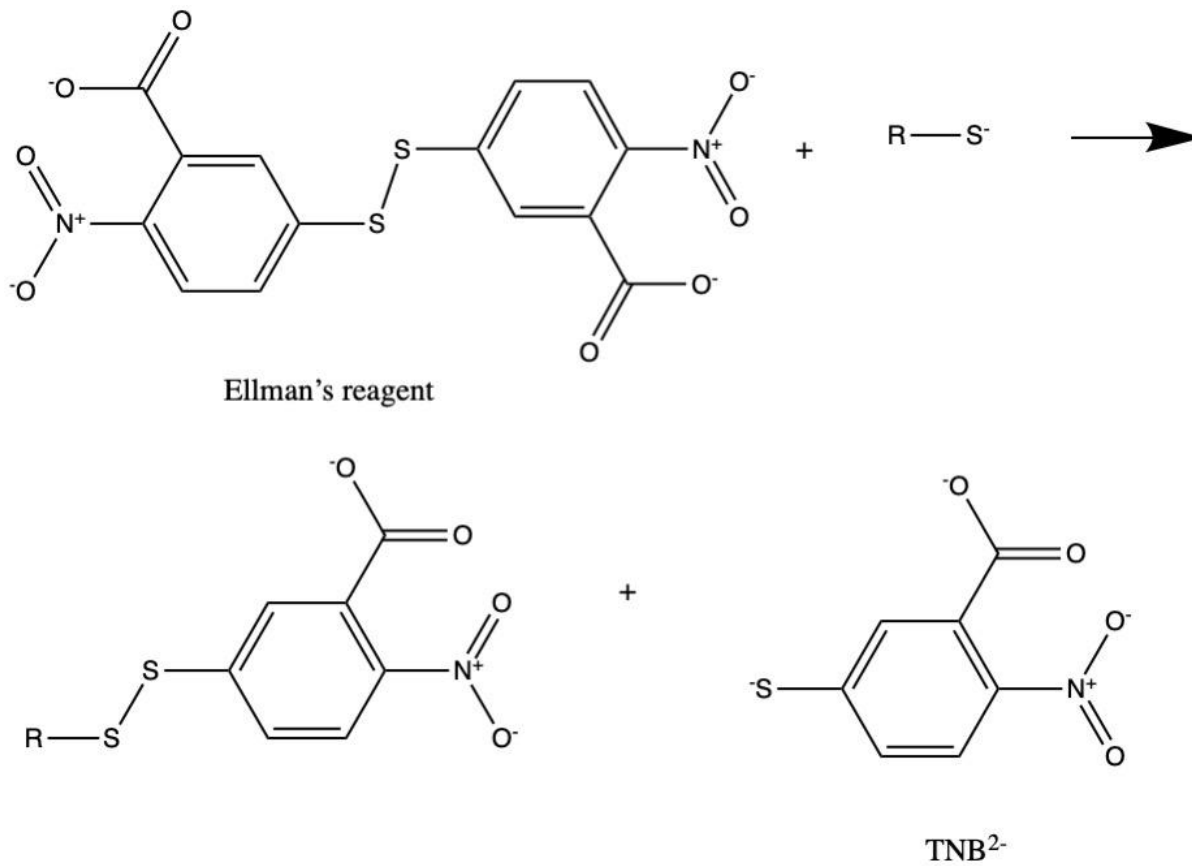
Figure 4.4 Illustration of Ellman's reagent reaction mechanism for forming TNB anions.

4 mg of Ellman's reagent was dissolved in 1 ml of buffer solution to make Ellman's reagent solution. Then 50 μl of Ellman's reagent solution was mixed with 2.5 ml of buffer solution, and 250 μl of each sample solution was added, with 250 μl of buffer solution for the blank. Samples were allowed to react with Ellman's reagent at room temperature for 15 minutes, and three types of samples were tested: gelatin solution (5% w/v) without Traut's reagent added, gelatin solution mixed with Traut's reagent for an hour but without sonication, and microbubble solution. Each sample was measured twice and the result with error bars is shown below in Fig 4.5.
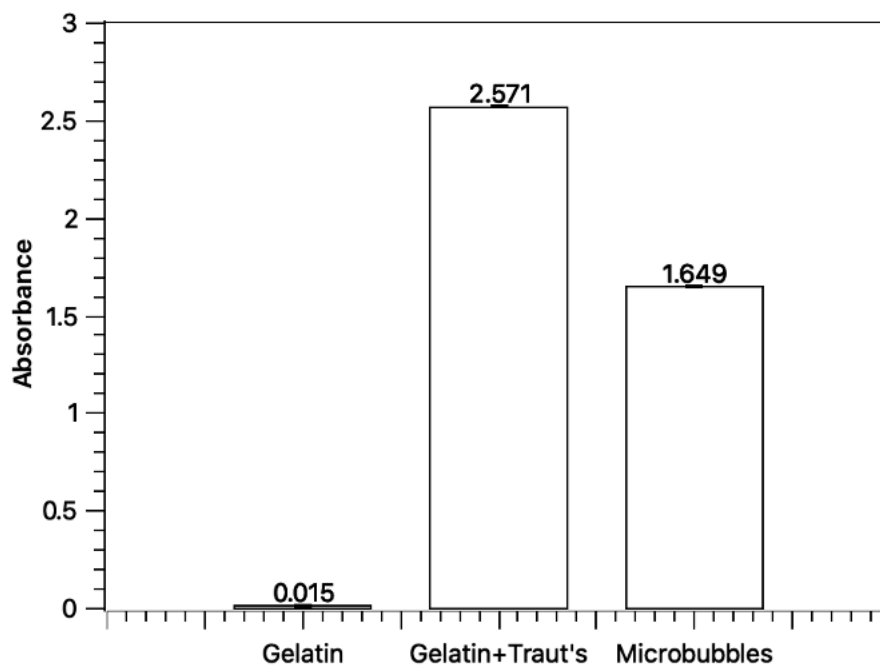
Figure 4.5 Absorption of different materials at 412 nm by Shimadzu UV-3600.

Considering gelatin only has a trace amount of cysteine, it's not surprising that initially not much absorbance was detected. After gelatin reacted with Traut's reagent, a lot of free thiol groups were added onto the gelatin surface, and the absorbance went up to 2.571 as shown in Figure 4.5; then during the sonication process microbubbles were formed and some free thiol groups became disulfide bonds, so the absorbance went down slightly to 1.649.

Considering molar absorptivity $E = \frac{A}{bc}$, where A is absorbance, b is path length in centimetres (1cm in this case), c is concentration, the absorbance value has a linear correlation with the free thiol concentration. So it can be estimated that a total of $\frac{2.571-1.649}{2.571} = 35.9\%$ free thiol groups were consumed to form disulfide bonds.

4.3 Digital images

Digital images were obtained from a Keyence VHX-700F digital microscope to help identify specific regions where microbubbles were concentrated on the wafer to provide guidance for further SEM imaging. Digital images can also provide a good holistic view of microbubbles and protein aggregates. Samples were made by using a pipette to withdraw a tiny aliquot of microbubble solution first and then it was dropped on a clean silicon wafer and left to dry overnight. Wafers were then put under the digital microscope's 1000x lens. Figure 4.6 and figure 4.7 below showed groups of microbubbles with a diameter from less than 1 μm to around 8 μm. And it can be clearly observed they have spherical shapes and differ significantly from the gelatin aggregates that are shown in Figure 4.8, which appear to be in irregular shapes.
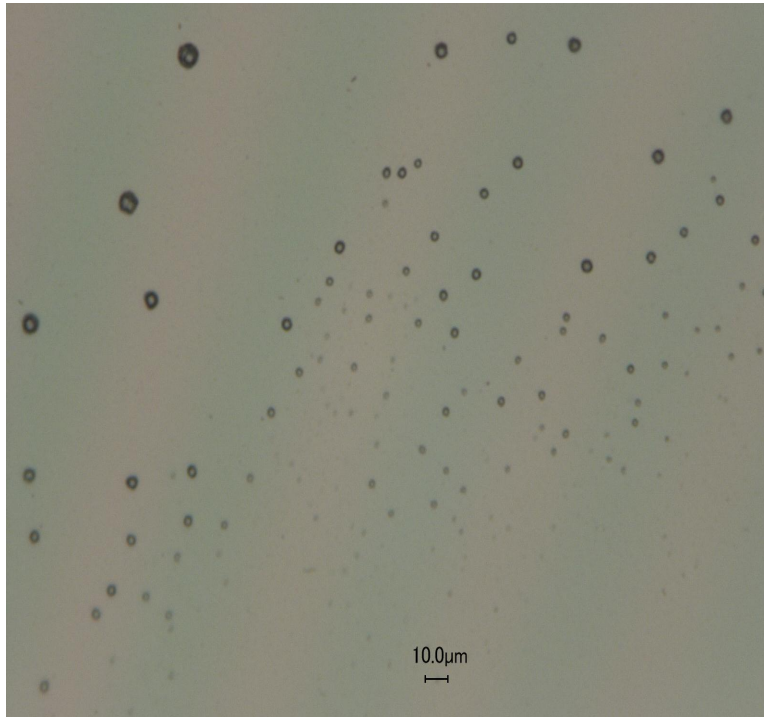
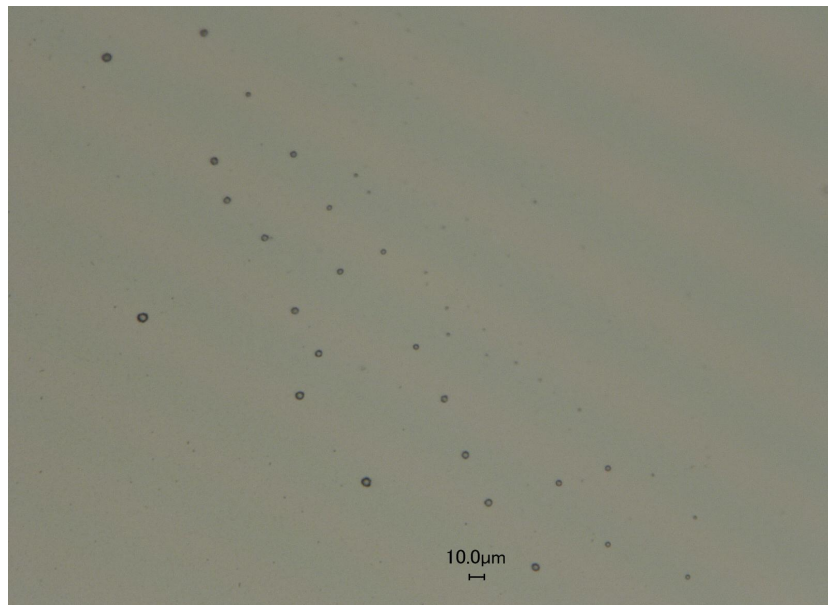Figure 4.6 Digital image 1 of gelatin-shelled microbubbles.

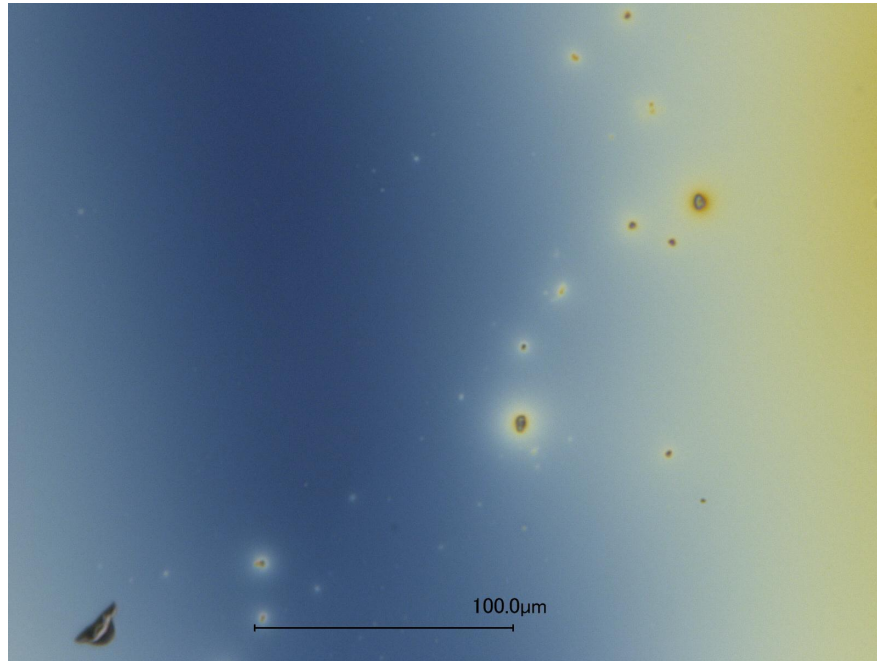Figure 4.7 Digital image 2 of gelatin-shelled microbubbles.

Figure 4.8 Digital image of gelatin aggregates.

4.4 SEM

4.4.1 Morphology

To further study the morphology of the microbubbles, SEM images were obtained using a sigma FE-SEM. The samples were prepared as described in 3.2; in short, they were left to evaporate overnight on wafers, and then sputtered with 5 nm of carbon. An in-lens detector was used and the SEM was operated at an electron high tension (EHT) of 5 kV. Evaporation was chosen in favour of freeze-drying so there is no additional deposition happening on the surface, as a result the surface of the microbubbles is rougher than those made from freeze-drying, in agreement with the previous research[75]. Images from the SEM were shown below. Figure 4.9 showed a more detailed view of the same region as in Figure 4.7; and Figure 4.10 and 4.11 showed one individual microbubble (with a diameter of around 1.2 μm) and its surface structure. Larger

microbubbles appear to be more stable than some smaller microbubbles, as most microbubbles with a diameter less than 800nm appeared to have collapsed as shown in Figure 4.12. Most of them still retain a somewhat round shape but the air has escaped from the microbubbles, leaving just a 'ring' of gelatin. Two possible reasons may contribute to the collapse of smaller microbubbles: first, smaller microbubbles have higher Laplace pressure. According to the Young-Laplace equation, assuming it's a perfect sphere, $\Delta P = 2\gamma/R$, so the smaller the R is, the higher the pressure, and the pressure may cause the microbubble to shrink or collapse. Second, smaller microbubbles have fewer crosslinked gelatin molecules on its surface, which may cause the shell to be less stable than those formed with more crosslinked gelatin molecules. Larger microbubbles however, are generally very stable, they may go through initial shrinkage within the first 24 hours, but afterwards their sizes remain mostly unchanged even after two weeks.
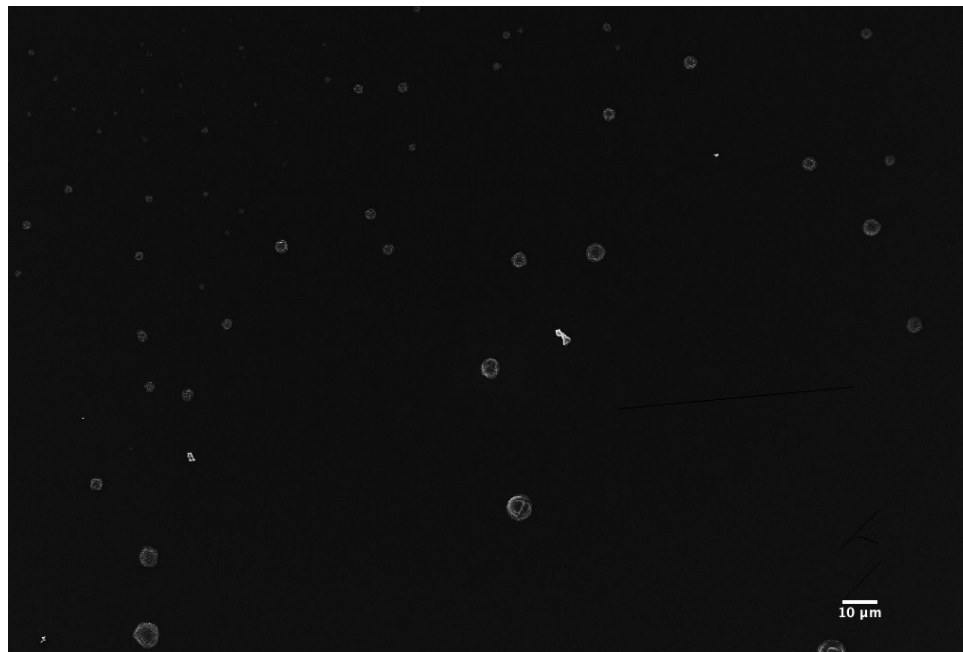

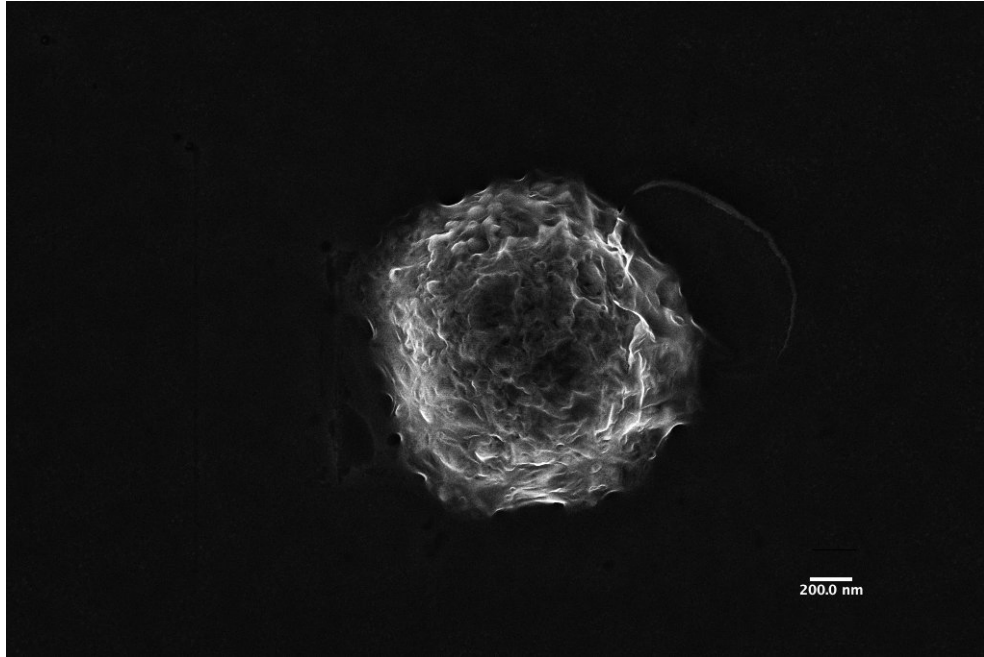Figure 4.9 Overview of gelatin-shelled microbubbles.

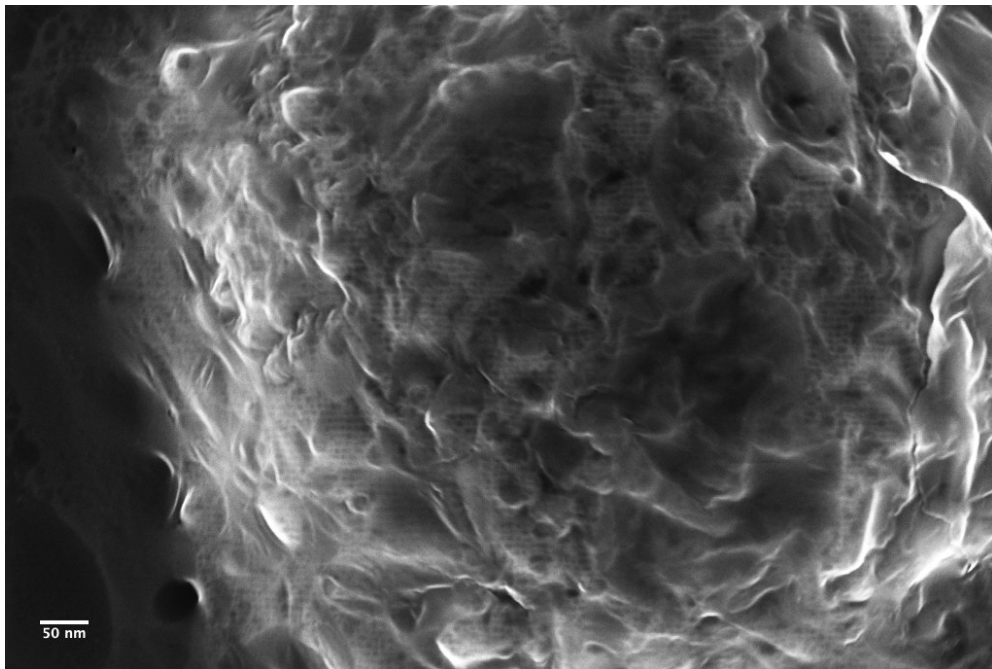Figure 4.10 FE-SEM image of a gelatin-shelled microbubble.

Figure 4.11 FE-SEM close-up image of a gelatin-shelled microbubble.
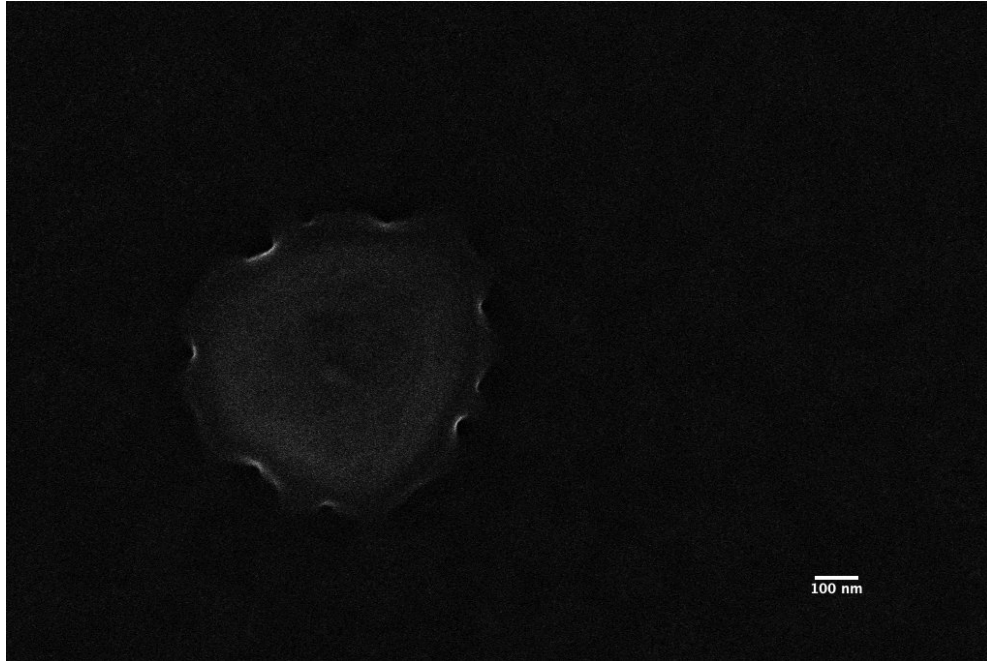
Figure 4.12 FE-SEM image of a collapsed microbubble.

4.4.2 Shell thickness

To study the shell thickness of the microbubbles, a cross-section of the gelatin-shelled microbubbles was needed; and ultra-fine sandpapers were used to break the microbubbles[75]. The samples were prepared the same way as before, a droplet was left on the wafer overnight to evaporate so microbubbles can stick to the wafer surface, and then the wafer surface was carefully and lightly sanded to break the microbubbles. 5 nm of carbon was coated onto the samples to increase their conductivity; afterwards SEM images were obtained using an electron high tension (EHT) of 5 kV. One particular thing to note is that as is shown below in Fig 4.13-4.15, even when SEM was adjusted properly, the cross-section SEM images appeared to be out of focus and not as clear as ones of intact microbubbles. A possible reason is that the sanding process made the surface uneven as a whole, and this made it very difficult to focus on the

microbubbles. The uneven surface may also make it harder for carbon to be coated uniformly and that may affect the image quality as well. Those images were then analyzed using ImageJ; for every image three lines were drawn from the outside edge of the shell to the inside edge of the shell and the average shell thickness was calculated to be about 175 nm (0.175 μm).

Figure 4.13 Shell thickness of FE-SEM image 1; the arrows show the microbubble shell; the average shell thickness of the bubble shown above is 153 nm.
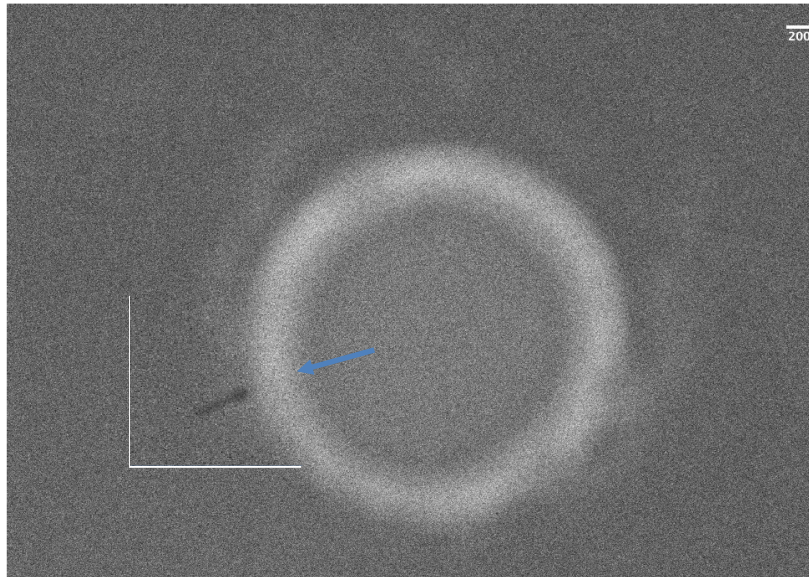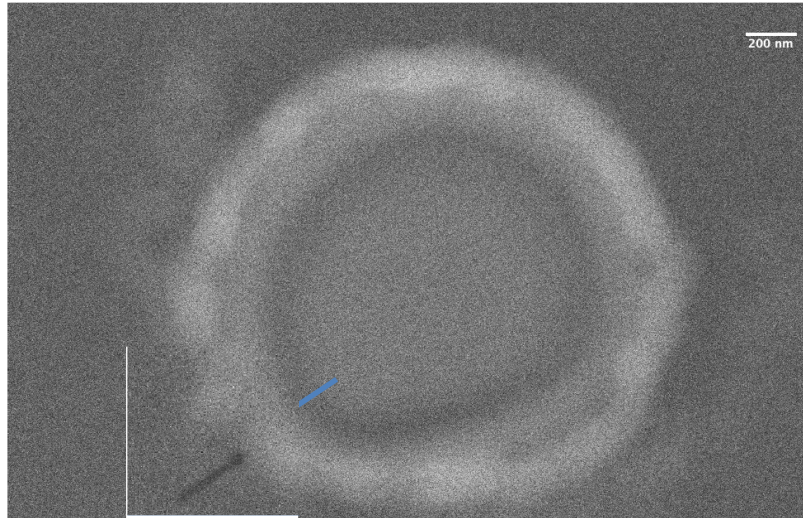
Figure 4.14 Shell thickness FE-SEM image 2; the arrows show the microbubble shell; the average shell thickness of the bubble shown above is 191 nm.
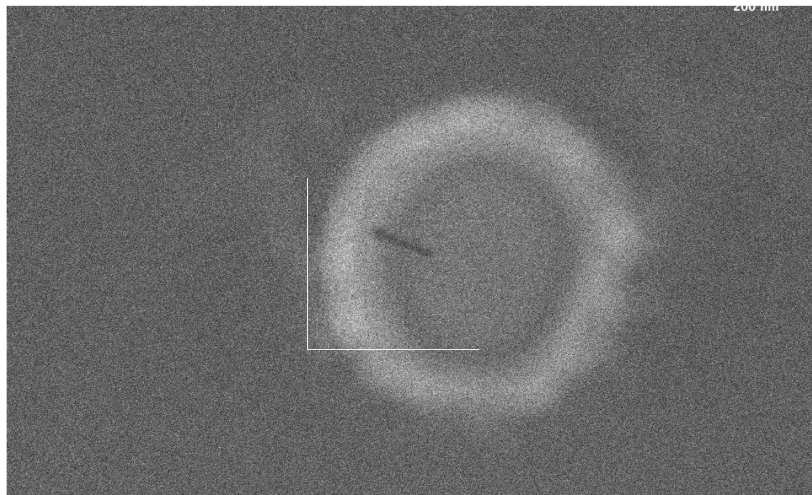

Figure 4.15 Shell thickness FE-SEM image 3; the arrows show the microbubble shell; the average shell thickness of the bubble shown above is 181 nm.

4.5 QCM-D

QCM-D experiments were carried out to test the reactivity of the gelatin-shelled microbubbles. Microbubble solutions were run through QCM sensors, while adsorption and dissipation were monitored. As explained in Chapter 3, according to the Sauerbrey equation, a decline in frequency and an increase in dissipation mean the occurrence of adsorption. Alumina and silica sensors were used to detect the electrostatic interactions between the sensors and the amine or carboxyl groups of the microbubble shell, and a gold sensor was used to detect the reactivity of thiol groups through the gold-thiol bonding effect. pH was selected to magnify the interactions, considering microbubbles have an IEP of around 4.5[70], which carry a net positive charge at pH 4, and a net negative charge at pH 6. As illustrated in Fig 4.16, at pH 6, the negatively charged microbubbles and positively charged alumina sensor can interact strongly with each other; and similarly, pH 4 condition favours the interaction between positively charged microbubbles and negatively charged silica sensor. Therefore, microbubble solutions were adjusted to pH=4 for silica sensor measurement and pH=6 for alumina sensor measurement. The interaction between thiol groups and gold is very strong and pH 6 is used to mitigate the possibility of electrostatic interactions between microbubbles and gold (IEP=5.2)[76] because both materials carry negative charges at pH 6. Background solutions were adjusted to the same pH.
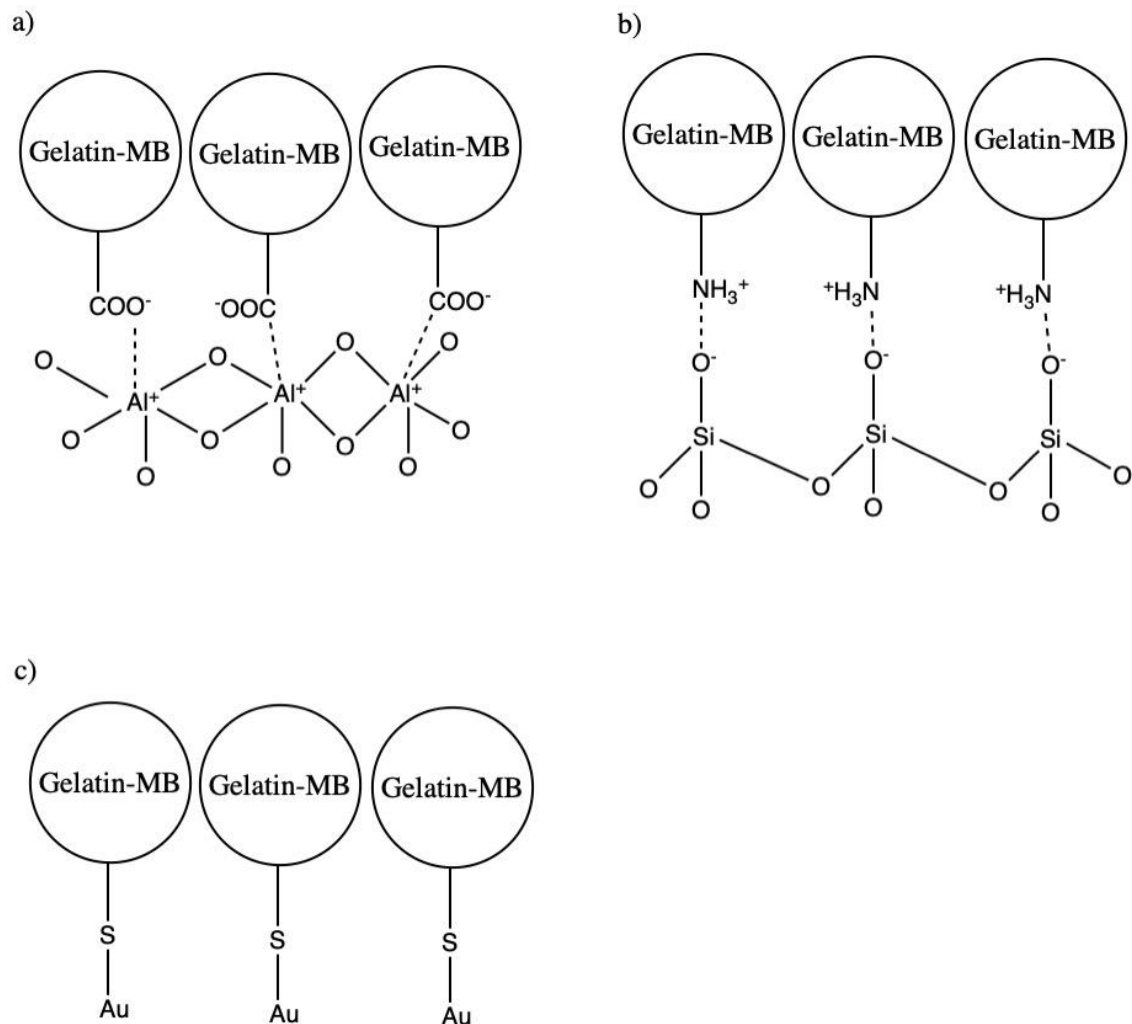
Figure 4.16 Interactions between gelatin-shelled microbubbles and various sensors; a) gelatin-shelled microbubbles interact with positively charged alumina sensor at pH 6; b) gelatin-shelled microbubbles interact with negatively charged silica sensor at pH 4; c) gelatin-shelled microbubbles interact with a gold sensor at pH 6 through Au-S bonding.

All samples were injected at a rate of 50 ul/min, and the frequency change and dissipation were measured by QCM-D. As is shown in figure 4.17, 4.19 and 4.20, after microbubble solutions were injected, there was a significant drop in frequency and a rise in dissipation, confirming the adsorption of microbubbles on the surface of the sensors. After a while, the frequency plateaued

with some very minor zig-zag fluctuations, showing an equilibrium being reached between the microbubble solutions and the sensor surface. Solutions kept going through the sensors at a constant rate; new microbubbles in the solution got attached to the surface while loosely bonded microbubbles were washed off the surface. Afterwards, sensors were rinsed off with the background solution, and the frequency rose as a result of some loosely bonded microbubbles being rinsed off the surface, but there remained a large frequency drop when compared to the starting point, confirming most microbubbles remained attached to the sensors.

As there are potentially unreacted gelatin proteins left in the microbubble solution, one may argue that all the frequency change was from the leftover gelatin. So an additional adsorption experiment was carried out on the silica sensor with gelatin solution that had reacted with Traut's reagent but hadn't been sonicated. The result is shown in Figure 4.18. The frequency drop for the gelatin solution was around 84 Hz, and the frequency drop for microbubble solution was around 74 Hz. That means the majority of all amino groups are still functional. Considering that the concentration of the leftover gelatin is significantly lower than the original gelatin solution, it can be concluded that the majority of the frequency drop and adsorption came from microbubbles. Furthermore, more microbubbles actually remained on the sensor surface after it was rinsed with a background solution. The fact that microbubbles retain the reactivity of their functional groups is very important, as they pave the way for promising applications such as drug delivery and wastewater treatment.
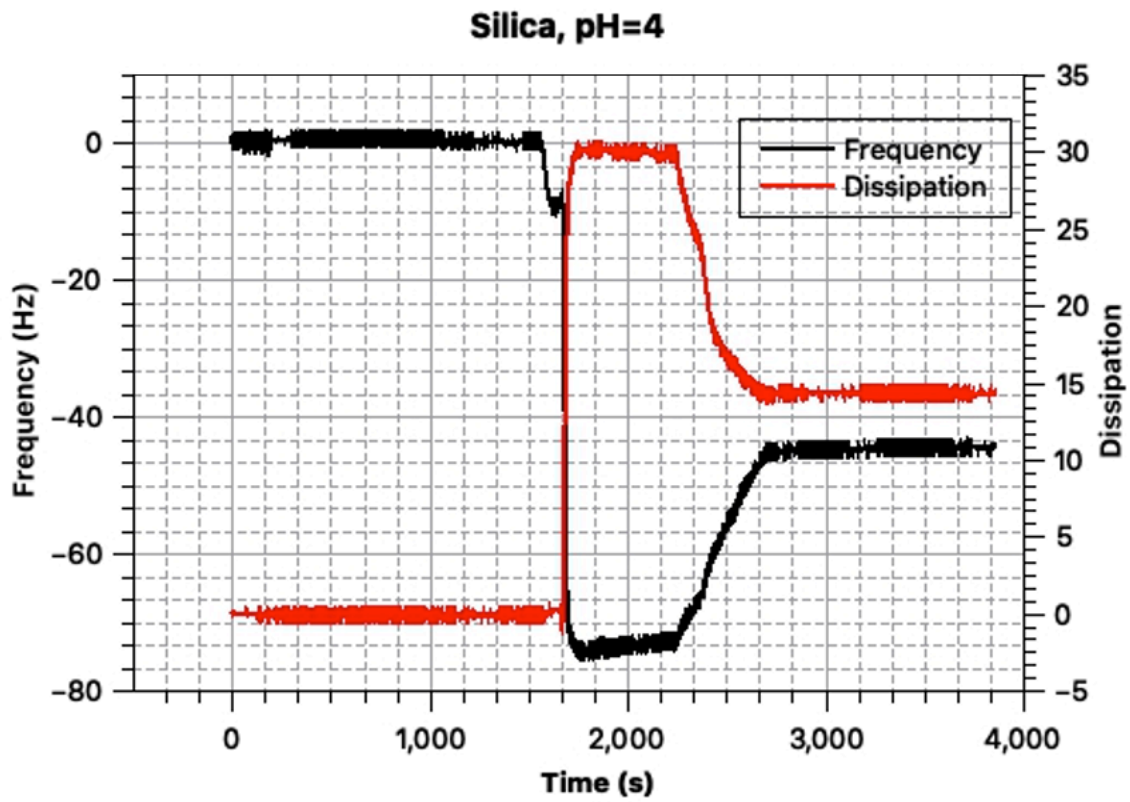
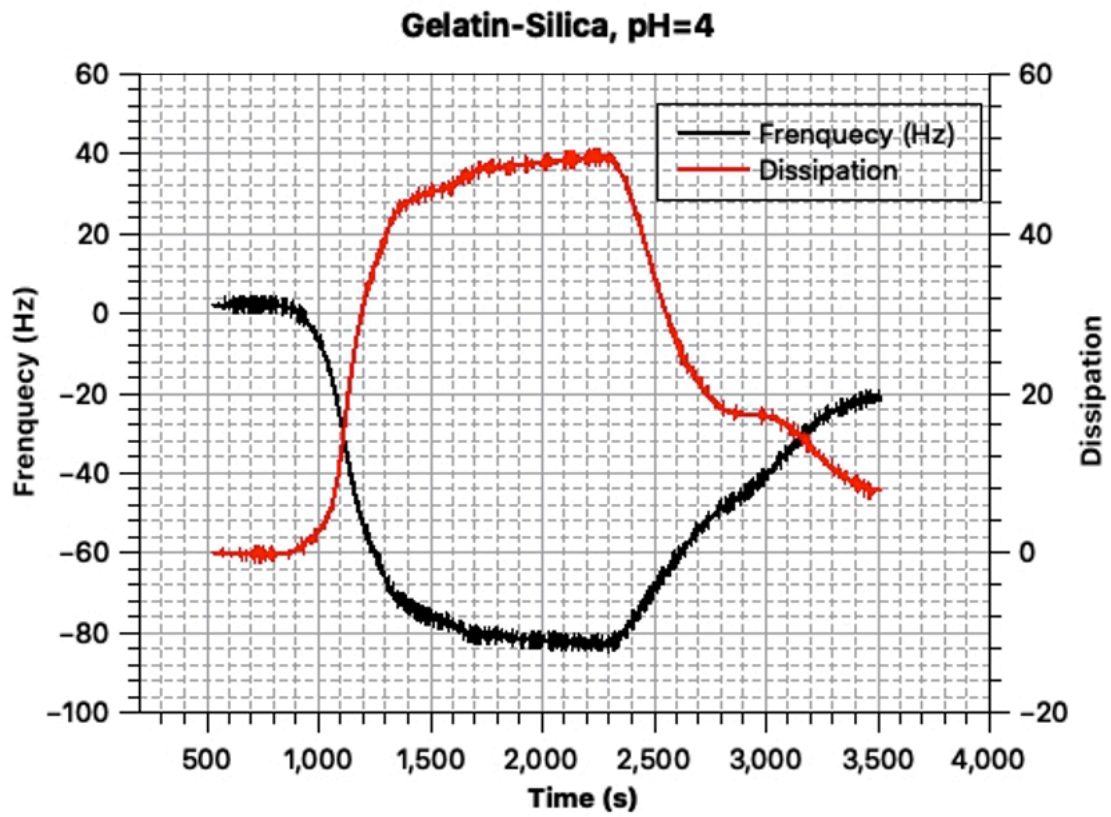Figure 4.17 Adsorption of microbubble solution on silica QCM-D sensor at pH 4.

Figure 4.18 Adsorption of gelatin solution on silica QCM-D sensor at pH 4.
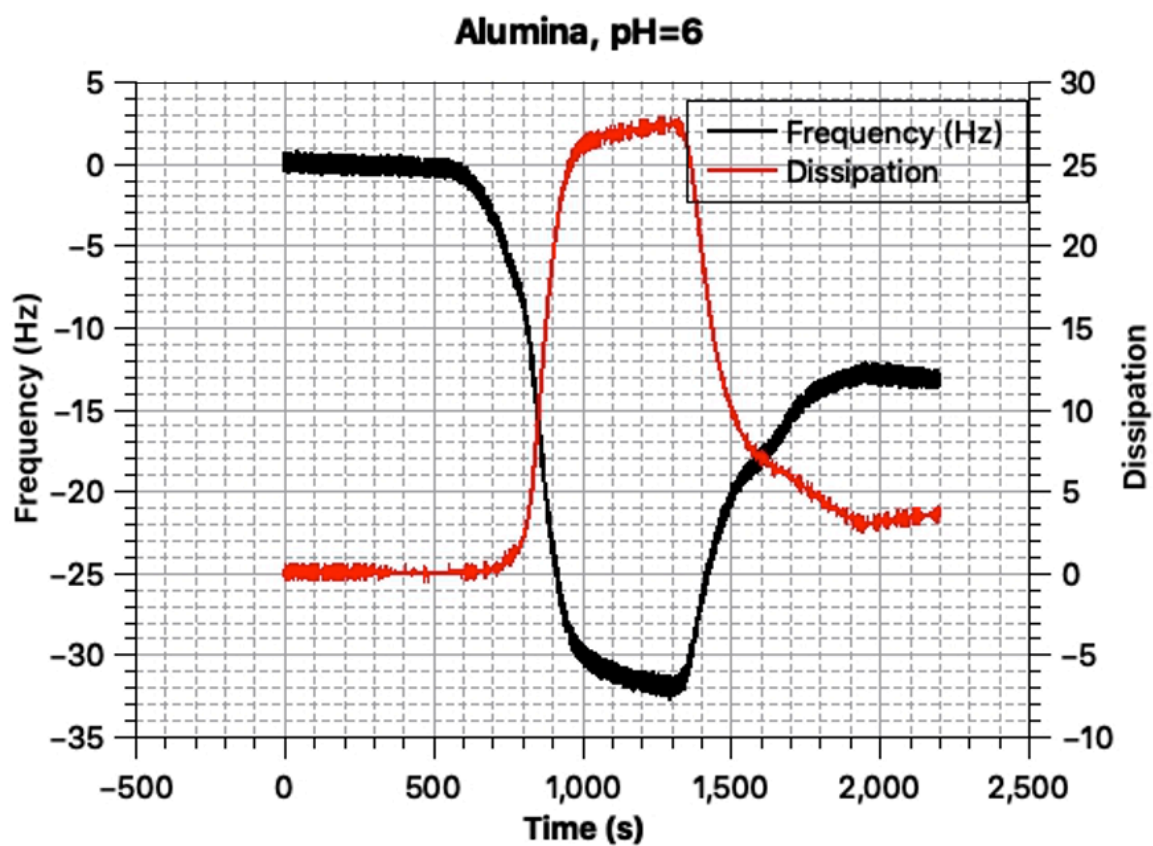
Figure 4.19 Adsorption of microbubble solution on alumina QCM-D sensor at pH 6.
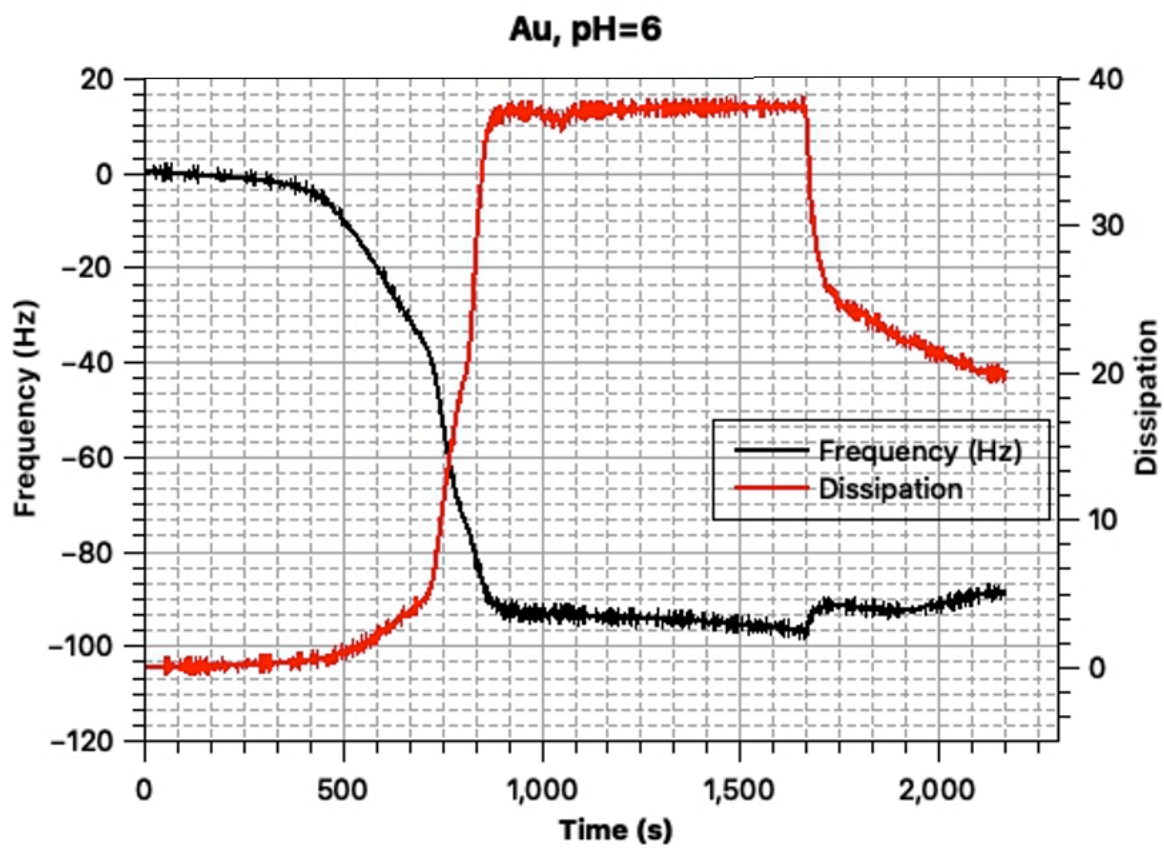
Figure 4.20 Adsorption of microbubble solution on gold QCM-D sensor at pH 6.

Chapter 5 Tailoring the properties of microbubbles

5.1 Introduction

Size is arguably the most important property of microbubbles; it has a direct impact on the viability of potential applications. For example, in drug delivery, microbubbles need to be small enough to pass through membranes and vessel walls[77], and they need to be big enough to maintain a high degree of echogenicity. Therefore, it's crucial to study the effects of various experimental parameters on the size distribution of microbubbles. And with these results, we can gain better control of the size of microbubbles by adjusting those parameters. In this chapter, 5 different parameters and their effects on microbubble size will be studied and discussed, including gelatin concentration, pH, gelatin to Traut's reagent ratio, sonication time and amplitude. They are selected based on the experimental conditions that previous researchers have identified to have a major effect on the size distribution of microbubbles[41].

5.2 The effects of gelatin concentration on the size of microbubbles

In the previous chapter, all the gelatin solutions used were 5% w/v. Additional gelatin solutions with a gelatin concentration of 1%, 2% and 10% were prepared, and all other experimental parameters remained the same. Microbubbles were generated with an initial pH = 8, a 1:20 ratio of gelatin to Traut's reagent, and a sonication period of 45s at 25%. The size distribution data were obtained using a Malvern Zetasizer Nano and the result is shown in Fig 5.1:
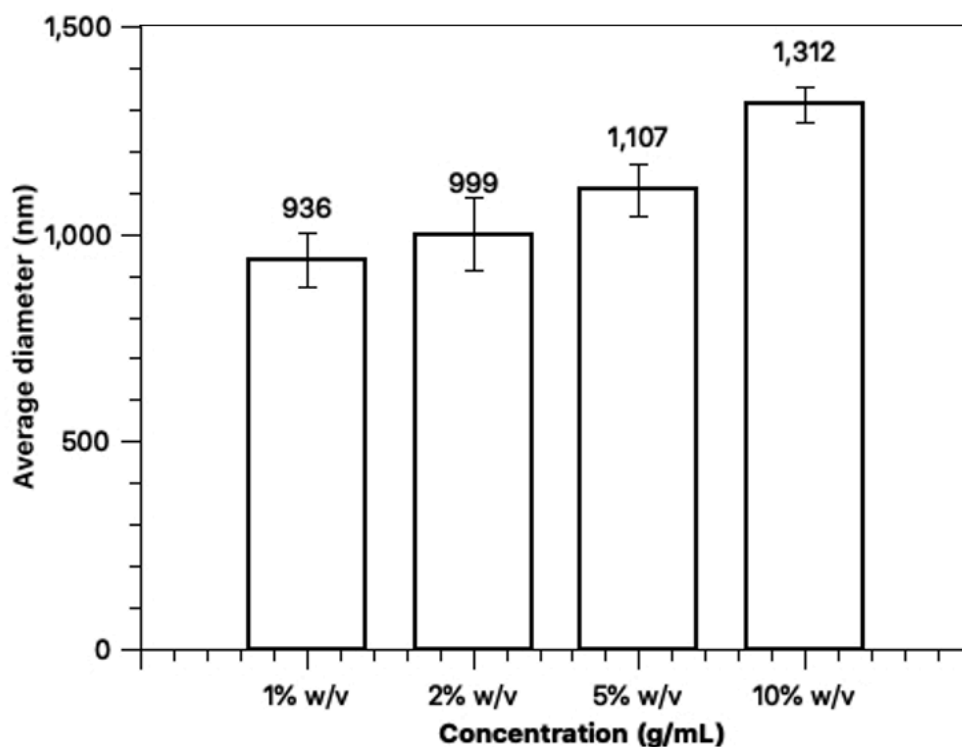
Figure 5.1 Microbubble size as a function of gelatin concentration.

It appears that the higher the initial concentration of gelatin, the larger the average size of the microbubbles. Although the increase isn't very dramatic, the overall trend is quite clear. Considering that the microbubbles were generated on the air-water interface, higher gelatin concentration means more gelatin molecules on the surface. So during the sonication period, more gelatin molecules were available to form the rigid shell for microbubbles in higher concentration samples than lower ones, which means more gelatin molecules were going to be cross-linked to make the shell more stable; so larger microbubbles were more likely to survive.

5.3 The effects of pH on the size of microbubbles

All samples used had a gelatin concentration of 5% w/v, a gelatin to Traut's reagent ratio of 1:20, and they were all sonicated at 25% for 45s. Previous research showed that pH can potentially have an impact on the size of the microbubbles[75,78], but its exact impact remains inconclusive. Here samples with an initial pH ranging from 4 to 10 were examined and the result is shown below in Fig 5.2.
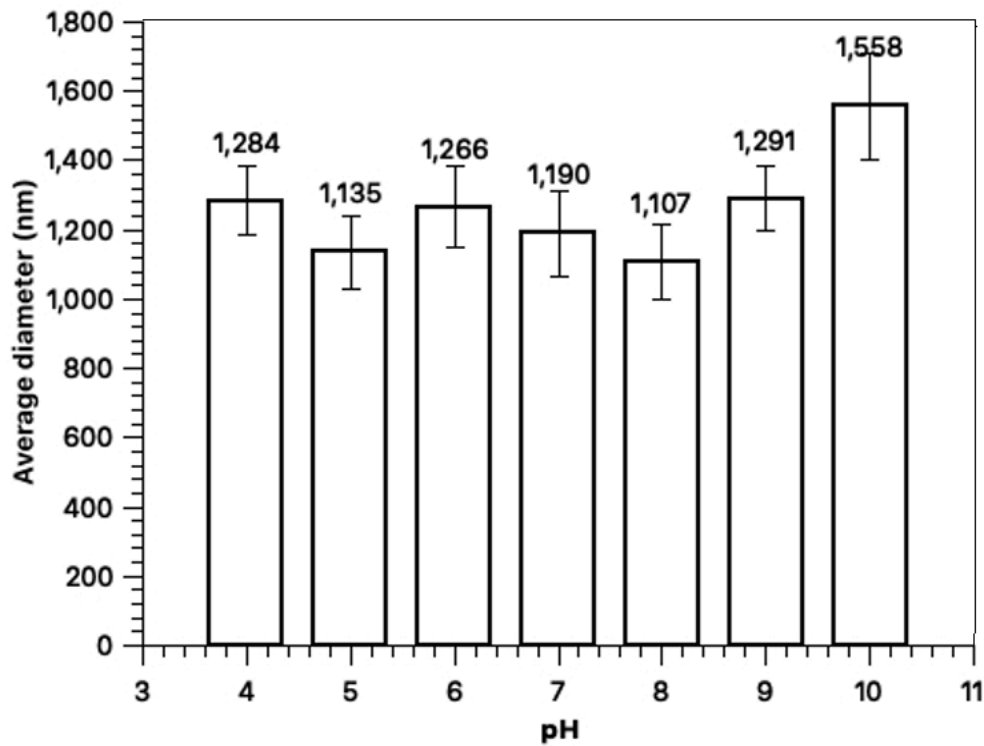
Figure 5.2 The effects of pH on microbubble size.

It appears that pH doesn't have a clear impact on the size of microbubbles, when pH is between 4 and 9 they all yield a similar size and at pH=10, a slightly larger bubble size. Some previous researchers found that microbubbles were more stable when pH was around the isoelectric point (pH around 5)[75,78]; but in the case of gelatin microbubbles, the size remains almost the same. The reason may be that the conformational change of gelatin molecules due to different pH is not significant enough to have a tangible effect on the size of the microbubbles, and pH alone doesn't have a very significant influence on the sonication synthesis process either.

5.4 The effects of the ratio of gelatin and Traut's reagent on the size of microbubbles

The use of Traut's reagent is the most important step for the synthesis of microbubbles, and the ratio of gelatin to Traut's reagent is directly related to the extent of thiolation of gelatin; therefore it can have a major impact on the size of the microbubbles. Samples with a ratio of gelatin to Traut's reagent at 1:1, 1:5, 1:10, 1:20 and 1:50 were prepared, all with a concentration of gelatin at 5% w/v, pH = 8 and they were sonicated at 25% for 45s. The result is shown below in Fig 5.3.
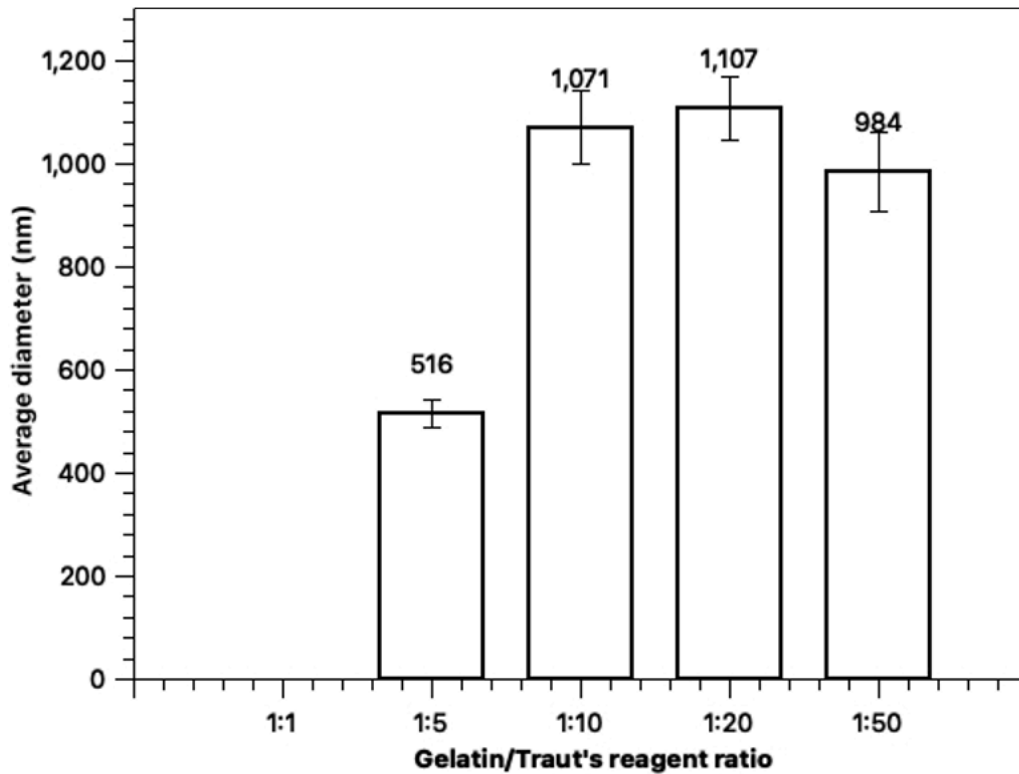
Figure 5.3 The effects of gelatin/Traut's reagent ratio on microbubble size.

When the ratio was 1:1, the result was simply too unreliable so it's not included in the chart.

There might be very few microbubbles that were generated when the ratio was 1:1 so it's masked

by a large number of protein particles during the measurement. Considering that gelatin has very

few natural thiol groups, it's unsurprising that not many microbubbles can be synthesized when

Traut's reagent is not adequate. As the relative amount of Traut's reagent goes up, it can be

observed that the average size of microbubbles first goes up, and then goes down at a high ratio.

A possible explanation of this result is that there are two factors affecting the size of

microbubbles here. First, when there is less Traut's reagent, there are only a few thiol groups

being added onto gelatin molecules that it's very difficult to have them crosslinked with each

other to form a rigid and stable shell for the microbubbles; Second, when there is too much

Traut's reagent, and consequently a large number of thiol groups on the gelatin molecules, their

structure can get too stretched out; and all the added functional groups can take up a large

amount of space around the molecule and limit the orientation of the crosslinking process,

therefore hindering the formation of large microbubbles. It can be seen that the largest

microbubbles can be obtained at around 1:10 to 1:20 ratio because it's a good balance point

between the two aforementioned factors.

5.5 The effects of sonication time and amplitude on the size of microbubbles

Sonication time and amplitude can also affect the size of microbubbles; and a combination of the

two can be used as a convenient tool to tailor the size of the microbubbles on demand [41]. A 5%

w/v concentration, pH = 8 environments and 1:20 ratio were maintained throughout the

experiments and the results were shown below in Fig 5.4 and 5.5.
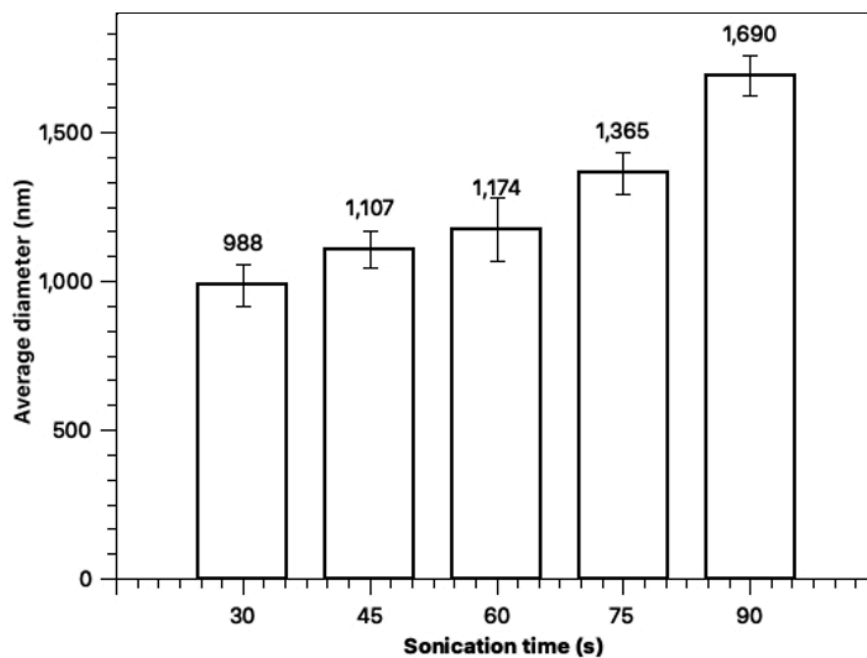
Figure 5.4 The effects of sonication time on the size of microbubbles.
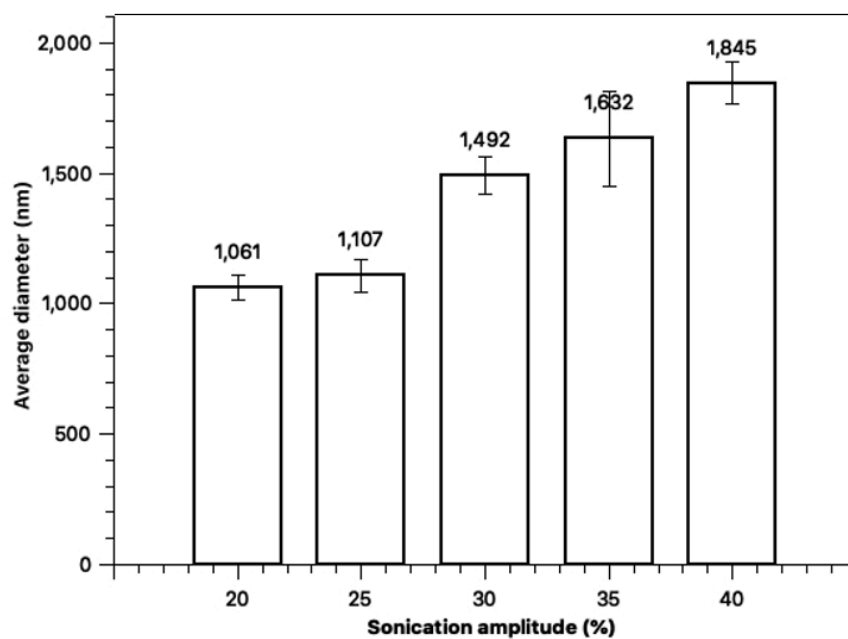
Figure 5.5 The effects of sonication amplitude on the size of microbubbles.

When compared to the other factors mentioned previously in the chapter, we can see both sonication time and amplitude have a larger impact on the size of microbubbles. In general, bubble size grows as time lengthens and amplitude increases, and potentially there are two reasons for it. First, as sonication time and amplitude increase, there can be more air being dissolved into the solution during the cavitation phase and subsequently getting encased in the gelatin shell; second, the larger force by the microtip of the dismembrator or the longer time under the acoustic force can increase the coalescence between smaller microbubbles to form bigger ones.

Chapter 6 A potential two-step approach to the synthesis of microbubbles

6.1 Introduction

In Chapter 4, the detailed process of gelatin microbubble synthesis with the help of Traut's reagent is discussed, and it is apparent that the introduction of thiol groups onto gelatin is the most crucial step in the process. The increased amount of thiol groups made cross-linking possible and thus increased the stability and life span of microbubbles. This can naturally lead to another hypothesis: if the amount of thiol groups on the surface of gelatin is further increased, it may lead to further increased stability and higher yield of microbubbles. The increased cross-linking means more a rigid shell, and it may prevent smaller microbubbles from bursting due to Laplace pressure.

Considering that Traut's reagent reacts with free amine groups, an increased amount of amine groups will translate to an increased amount of thiol groups. One way to do this is to follow the two-step process introduced by Duggan et al. to synthesize mucoadhesive thiolated gelatin[79]. First they aminated gelatin with ethylene diamine with the presence of crosslinker EDC (1-ethyl-3-(3-dimethylaminopropyl) carbodiimide); then they used Traut's reagent to thiolate the modified gelatin. It resulted in much more heavily thiolated gelatin molecules; so naturally it can potentially lead to more stable shells in gelatin microbubbles.

The significance of this potential two-step approach is not limited in the synthesis of gelatin-shelled microbubbles, even more importantly, it can pave the way for proteins with few natural

amine and thiol groups to act as microbubble shells. So far only very few proteins have been used as shells, but this two-step approach can be almost universally used towards most proteins; it means for drug molecules that can only bind with certain specific proteins. It's possible to build a drug delivery vehicle using those specific proteins with this two-step method. This will largely increase the pool of drug molecules that can be delivered using protein-shelled microbubbles, making a lot of previously impossible drug delivery system a reality.

6.2 Design of experiments of the two-step approach

20 ml of 5% w/v gelatin solution was prepared using PBS solution (pH adjusted to 8.0). 2.8 g of ethylenediamine was added to the solution and pH was then adjusted to 5, before adding 0.5 g of EDC. Then the mixture was left at room temperature with gentle stirring for 24 hours. The sample was then dialyzed using a 7K desalting column, freeze-dried and stored at 4 °C.

Afterwards, 200 mg of freeze-dried gelatin sample was dissolved in 20 ml of DI water, and then 20 times Traut's reagent was added. pH was adjusted to 5 and then the mixture was left at room temperature with gentle stirring for 24 hours. The sample was then dialyzed again and stored at 4 °C. The blank sample was prepared following the same steps except for no ethylene diamine and EDC. The reaction mechanism is shown below in Fig 6.1.

6.3 Quantification of thiol groups on microbubble surface
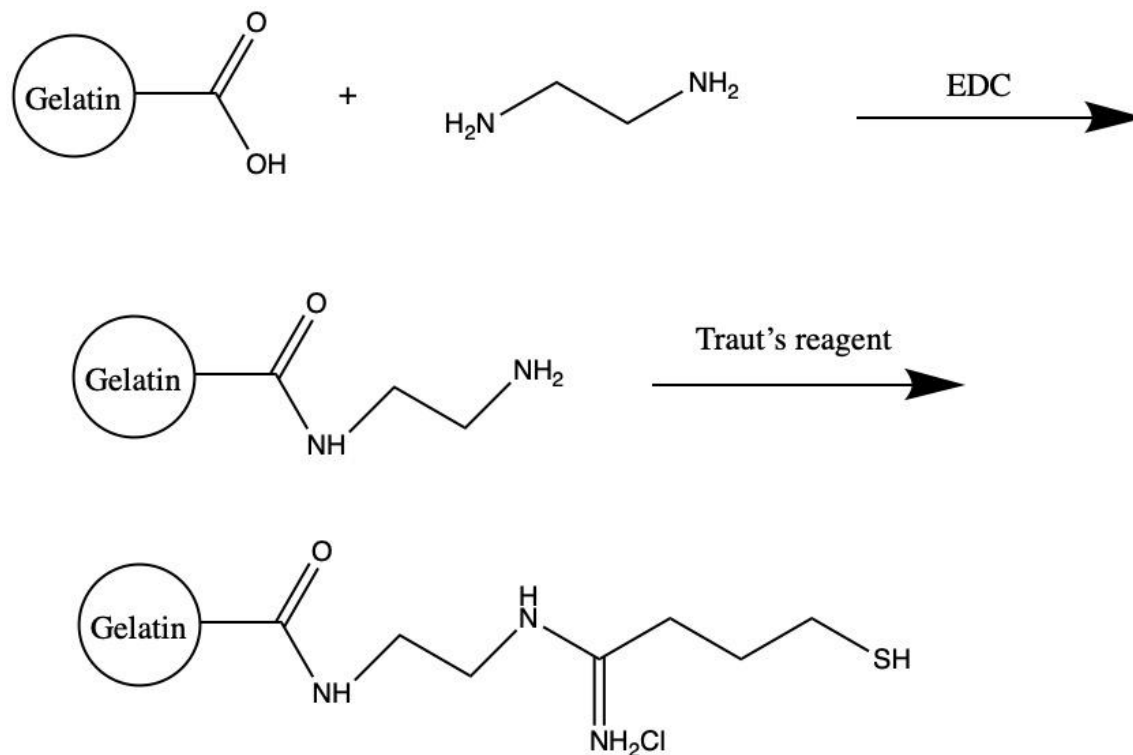
Figure 6.1 Two-step thiolation process for gelatin[79].

Similar to the process described in 4.2, Ellman's reagent was used for thiol group quantification. The absorption result is shown below in Figure 6.2. The amount of thiol groups on aminated gelatin is 8 times the amount on non-aminated gelatin (blank). It's very clear that the extra amine groups greatly increased the degree of thiolation of gelatin.
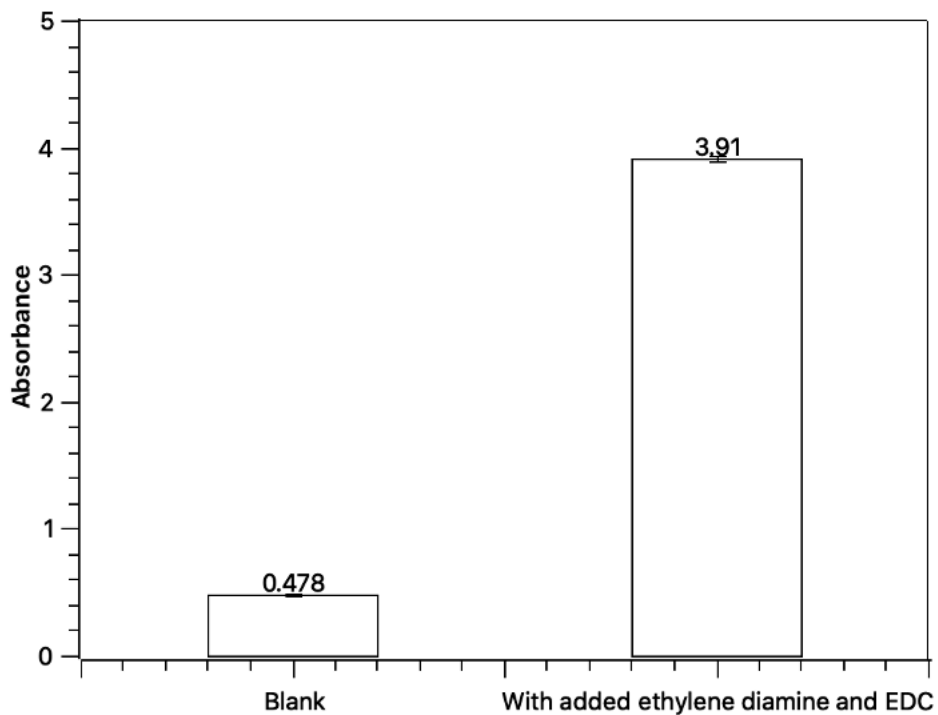
Figure 6.2 Absorption at 412 nm for quantification of thiol groups with Ellman's reagent.

6.4 Comparison of microbubble size

Both samples were sonicated at 25% amplitude for 45s to generate microbubbles. Afterwards, aqueous phases of the solutions were withdrawn using a pipette to new tubes and then stored at room temperature. After 24 hours the sizes of both samples were measured using a Zetasizer nano; and the result is shown in Fig 6.3. Each result is the average of three measurements of the same sample. The size of aminated gelatin shelled microbubbles was smaller than non-aminated ones, suggesting that the increased stability of the shell potentially protected smaller bubbles from collapsing. It's also possible that the additional thiol groups on the surface of gelatin clogged up space around the molecule and limited the orientation gelatin molecules can crosslink with each other, limiting the formation of larger microbubbles, which is similar to the result with

50 times molar excess of Traut's reagent as shown in Fig 5.3. Further research is still needed to study the exact reason for their size differences, but the significance of this preliminary exploration is that through this two-step process, microbubbles of a desirable size (around 1 μm in this case) can still be synthesized and this can open the door for other proteins with limited amine groups to act as microbubble shells.
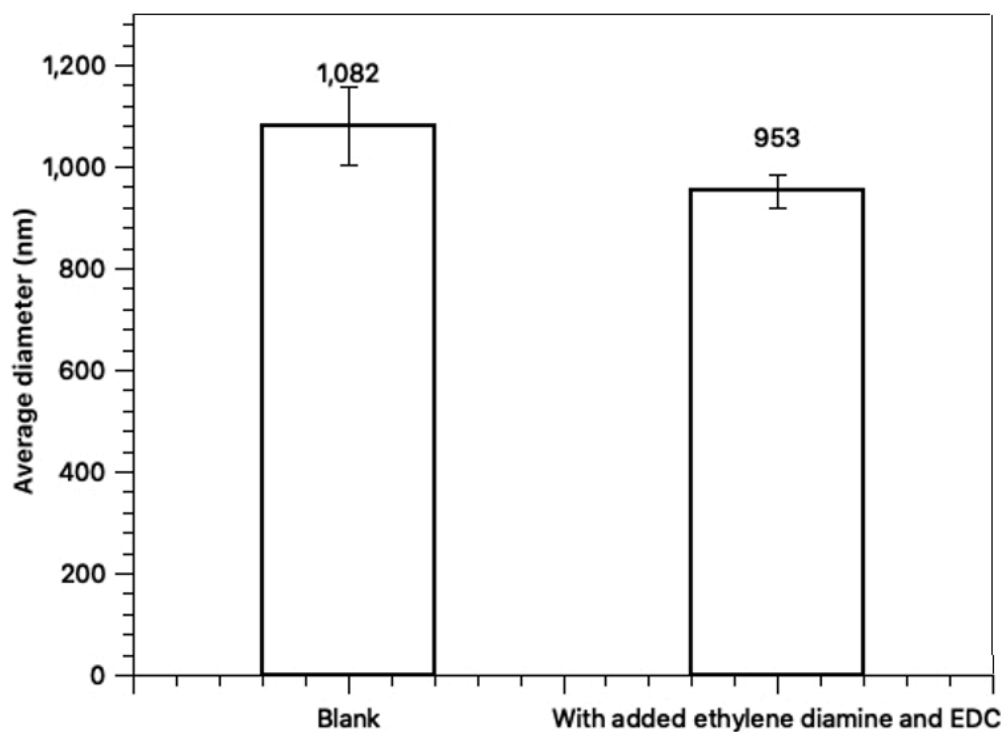
Figure 6.3 The sizes of microbubbles synthesized with and without amination process.

Chapter 7 Conclusion

In this thesis, a new approach to synthesizing gelatin-shelled microbubbles is introduced; those microbubbles are then characterized using techniques such as SEM, spectrophotometry, FTIR, dynamic light scattering, and QCM-D. The effects of various experimental parameters such as pH, sonication time and amplitude, gelatin concentration to Traut's reagent ratio, etc. were studied. And in the end a modification of the two-step method to improve the synthesis process was proposed with the potential of expanding this approach to much wider applications. Key findings can be summarized as follows:

1. Gelatin-shelled microbubbles can be successfully synthesized with the help of Traut's reagent; gelatin gets thiolated first and then the solution is sonicated at the water-air surface to form a cross-linking of disulphide bond S-S on the surface of microbubbles.

2. The synthesized microbubbles have a size of roughly 1100 nm in diameter with a shell thickness of about 175 nm. Smaller microbubbles seem to be unstable.

3. The carboxyl, amine and thiol groups on the bubble surface remain to be reactive as indicated by QCM-D results, which can potentially act as great binding sites for drug molecules.

4. Microbubble size increases as gelatin concentration, sonication time or amplitude increases. pH doesn't appear to have a tangible impact on microbubble sizes. Microbubble size first increases and then decreases as the ratio between Traut's reagent

and gelatin goes up. Adjusting those experimental parameters can help tailor the size of microbubbles to generate the most desirable microbubbles for future applications.

5. By using a two-step synthesis method, up to 8 times more thiol groups can be introduced onto gelatin. For proteins with limited natural thiol and amine groups, this two-step method can enable the successful thiolation process on protein, and it can expand the pool of potential proteins as microbubble shells to almost all types of proteins, greatly increasing the drug delivery viability.

Chapter 8 Future work

1. Multi-dimensional model for tailoring the size of microbubbles

   The effects of individual factors were investigated but with more dataset a multi-dimensional model can be built, with interactions between experimental parameters taken into account. Eventually the model can potentially predict the size of the microbubbles based on any given set of experimental parameters. This can be very useful in commercial applications considering different sized microbubbles are preferred based on specific applications; and this model can take all the parameters into consideration at the same time, increasing the accuracy of the prediction.

2. Using the two-step approach to synthesize microbubbles using proteins that are low in thiol and amine groups

   Gelatin experiments proved that the two-step approach can increase the thiolation degree of gelatin, but it still needs confirmation that this process can enable proteins that have very few thiol and amine groups to become thiolated and crosslinked to form microbubble shells. Proteins with zero or very few cysteine, lysine and arginine are good candidates for this research.

3. Drug loading experiments

   Although QCM-D experiments proved the reactivity of the functional groups, future experiments are still needed to test the drug loading process. The structural changes during the crosslinking process and the spatial limitation due to the newly introduced

thiol groups can potentially hinder their drug loading capabilities.

4. Non-biomedical applications

QCM-D confirmed the strong interaction between gelatin microbubbles and gold surface; so apart from apparent biomedical applications, other functions of the gelatin microbubbles can also be explored. As discussed in the literature review, potentially they can be used for wastewater treatment, especially absorbing heavy metal ions; they can also be used during the flotation process to collect fine metal particles.

References

1. Qin, S.; Caskey, C. F.; Ferrara, K. W. Ultrasound contrast microbubbles in imaging and therapy: physical principles and engineering. *Physics in Medicine and Biology* **2009***, 54*, 4621.

2. de Jong, N.; Cornet, R.; Lancée, C. T. Higher harmonics of vibrating gas-filled microspheres. Part one: simulations. *Ultrasonics* **1994***, 32*, 447-453.

3. Lindner, J. R. Microbubbles in medical imaging: current applications and future directions. *Nature Reviews Drug Discovery* **2004***, 3*, 527-533.

4. Hernot, S.; Klibanov, A. L. Microbubbles in ultrasound-triggered drug and gene delivery. *Advanced Drug Delivery Reviews* **2008***, 60*, 1153-1166.

5. Yalcin, T.; Byers, A.; Ughadpaga, K. Dissolved gas method of generating bubbles for potential use in ore flotation. *Mineral Processing and Extractive Metallurgy Review* **2002***, 23*, 181-197.

6. Veis, A. *The macromolecular chemistry of gelatin;* New York: Academic, 1964.

7. Elzoghby, A. O.; Samy, W. M.; Elgindy, N. A. Protein-based nanocarriers as promising drug and gene delivery systems. *Journal of Controlled Release* **2012***, 161*, 38-49.

8. Leo, E.; Angela Vandelli, M.; Cameroni, R.; Forni, F. Doxorubicin-loaded gelatin nanoparticles stabilized by glutaraldehyde: Involvement of the drug in the cross-linking process. *International Journal of Pharmaceutics* **1997***, 155*, 75-82.

9. Suslick, K. S.; Grinstaff, M. W. Protein microencapsulation of nonaqueous liquids. *Journal of*

the American Chemical Society **1990***, 112*, 7807-7809.

10. Janib, S. M.; Moses, A. S.; MacKay, J. A. Imaging and drug delivery using theranostic nanoparticles. *Advanced Drug Delivery Reviews* **2010***, 62*, 1052-1063.

11. Ferrara, K.; Pollard, R.; Borden, M. Ultrasound Microbubble Contrast Agents: Fundamentals and Application to Gene and Drug Delivery. *Annual review of biomedical engineering* **2007***, 9*, 415-447.

12. De Cock, I.; Zagato, E.; Braeckmans, K.; Luan, Y.; de Jong, N.; De Smedt, S. C.; Lentacker, I. Ultrasound and microbubble mediated drug delivery: Acoustic pressure as determinant for uptake via membrane pores or endocytosis. *Journal of Controlled Release* **2015***, 197*, 20-28.

13. Roovers, S.; Segers, T.; Lajoinie, G.; Deprez, J.; Versluis, M.; De Smedt, S. C.; Lentacker, I. The Role of Ultrasound-Driven Microbubble Dynamics in Drug Delivery: From Microbubble Fundamentals to Clinical Translation. *Langmuir* **2019***, 35*, 10173-10191.

14. Tzu-Yin Wang; Katheryne E. Wilson; Steven Machtaler; Jurgen K. Willmann Ultrasound and Microbubble Guided Drug Delivery: Mechanistic Understanding and Clinical Implications. *Current Pharmaceutical Biotechnology* **2013***, 14*, 743-752.

15. Tsutsui, J. M.; Xie, F.; Porter, R. T. The use of microbubbles to target drug delivery. *Cardiovascular ultrasound* **2004***, 2*, 23.

16. Ashokkumar, M.; Cavalieri, F. *Handbook of ultrasonics and sonochemistry;* Springer Reference: Singapore, 2016; pp 1075-1100.

17. Unger, E.; McCreery, T.; Sweitzer, R.; Caldwell, V.; Wu, Y. Acoustically Active

Lipospheres Containing Paclitaxel: A New Therapeutic Ultrasound Contrast Agent. *Investigative Radiology* **1998***, 33*, 886-892.

18. Miller, M. W. Gene transfection and drug delivery. *Ultrasound in Medicine & Biology* **2000***, 26*, S59-S62.

19. Nazari, A. M.; Cox, P. W.; Waters, K. E. Copper ion removal from dilute solutions using ultrasonically synthesised BSA- and EWP-coated air bubbles. *Separation and Purification Technology* **2014***, 132*, 218-225.

20. Sahu, S. K.; Agrawal, A.; Pandey, B. D.; Kumar, V. Recovery of copper, nickel and cobalt from the leach liquor of a sulphide concentrate by solvent extraction. *Minerals Engineering* **2004***, 17*, 949-951.

21. White, J. M.; Manning, R. A.; Li, N. C. Metal Interaction with Sulfur-containing Amino Acids. II. Nickel and Copper(II) Complexes1. *Journal of the American Chemical Society* **1956***, 78*, 2367-2370.

22. Nazari, A. M.; Cox, P. W.; Waters, K. E. Biosorptive flotation of copper ions from dilute solution using BSA-coated bubbles. *Minerals Engineering* **2015***, 75*, 140-145.

23. Xu, Q.; Nakajima, M.; Ichikawa, S.; Nakamura, N.; Shiina, T. A comparative study of microbubble generation by mechanical agitation and sonication. *Innovative Food Science and Emerging Technologies* **2008***, 9*, 489-494.

24. Meifang Zhou; Francesca Cavalieri; Muthupandian Ashokkumar Ultrasonic Synthesis and Characterisation of Polymer-Shelled Microspheres. In *Handbook of Ultrasonics and*

Sonochemistry; Ashokkumar, M., Ed.; Springer Science+Business Media Singapore, 2015; pp 1-27.

25. Mark W. Grinstaff; Kenneth S. Suslick Air-Filled Proteinaceous Microbubbles: Synthesis of an Echo-Contrast Agent. *Proceedings of the National Academy of Sciences of the United States of America* **1991**, *88*, 7708-7710.

26. Carter, D. C.; He, X. M.; Munson, S. H.; Twigg, P. D.; Gernert, K. M.; Broom, M. B.; Miller, T. Y. Three-dimensional structure of human serum albumin. *Science* **1989**, *244*, 1195-1198.

27. Suslick, K. S.; Grinstaff, M. W. Protein microencapsulation of nonaqueous liquids. *Journal of the American Chemical Society* **1990**, *112*, 7807-7809.

28. Touch, V.; Hayakawa, S.; Saitoh, K. Relationships between conformational changes and antimicrobial activity of lysozyme upon reduction of its disulfide bonds. *Food Chemistry* **2004**, *84*, 421-428.

29. Cavalieri, F.; Ashokkumar, M.; Grieser, F.; Caruso, F. Ultrasonic Synthesis of Stable, Functional Lysozyme Microbubbles. *Langmuir : the ACS journal of surfaces and colloids* **2008**, *24*, 10078-10083.

30. Cavalieri, F.; Micheli, L.; Kaliappan, S.; Teo, B. M.; Zhou, M.; Palleschi, G.; Ashokkumar, M. Antimicrobial and Biosensing Ultrasound-Responsive Lysozyme-Shelled Microbubbles. *ACS Applied Materials & Interfaces* **2013**, *5*, 464-471.

31. Vong, F.; Son, Y.; Bhuiyan, S.; Zhou, M.; Cavalieri, F.; Ashokkumar, M. A comparison of

the physical properties of ultrasonically synthesized lysozyme- and BSA-shelled microbubbles. *Ultrasonics - Sonochemistry* **2014**, *21*, 23-28.

32. Kwan, J. J.; Borden, M. A. Lipid monolayer collapse and microbubble stability. *Advances in Colloid and Interface Science* **2012**, *183-184*, 82-99.

33. Sirsi, S. R.; Borden, M. A. Microbubble compositions, properties and biomedical applications. *Bubble Science, Engineering & Technology* **2009**, *1*, 3-17.

34. Rubino, O. P.; Kowalsky, R.; Swarbrick, J. Albumin Microspheres as a Drug Delivery System: Relation among Turbidity Ratio, Degree of Cross-Linking and Drug Release. *Pharmaceutical research* **1993**, *10*, 1059-1065.

35. Chen, G. Q.; Lin, W.; Coombes, A. G. A.; Davis, S. S.; Illum, L. Preparation of Human Serum Albumin Microspheres by a Novel Acetone-Heat Denaturation Method. *Journal of Microencapsulation* **1994**, *11*, 395-407.

36. Keller, M. W.; Glasheen, W.; Kaul, S. Albunex: A Safe and Effective Commercially Produced Agent for Myocardial Contrast Echocardiography. *Journal of the American Society of Echocardiography* **1989**, *2*, 48-52.

37. Chen, Johnny L.|Dhanaliwala, Ali H.|Dixon, Adam J.|Klibanov, Alexander L.|Hossack, John A Synthesis and Characterization of Transiently Stable Albumin-Coated Microbubbles via a Flow-Focusing Microfluidic Device. *Ultrasound in Medicine & Biology* **2014**, *40*, 400-409.

38. Upadhyay, A.; Dalvi, S. V.; Gupta, G.; Khanna, N. Effect of PEGylation on performance of protein microbubbles and its comparison with lipid microbubbles. *Materials Science &*

Engineering C **2017**, *71*, 425-430.

39. Rovers, T. A. M.; Sala, G.; van der Linden, E.; Meinders, M. B. J. Temperature is key to yield and stability of BSA stabilized microbubbles. *Food Hydrocolloids* **2016**, *52*, 106-115.

40. Avivi, S.; Gedanken, A. S–S bonds are not required for the sonochemical formation of proteinaceous microspheres: the case of streptavidin. *Biochemical journal* **2002**, *366*, 705-707.

41. Zhou, M.; Cavalieri, F.; Ashokkumar, M. Tailoring the properties of ultrasonically synthesised microbubbles. *Soft Matter* **2011**, *7*, 623-63.

42. Korpanty, G.; Grayburn, P. A.; Shohet, R. V.; Brekken, R. A. Targeting vascular endothelium with avidin microbubbles. *Ultrasound in Medicine & Biology* **2005**, *31*, 1279-1283.

43. Singhal, S.; Moser, C. C.; Wheatley, M. A. Surfactant-stabilized microbubbles as ultrasound contrast agents: stability study of Span 60 and Tween 80 mixtures using a Langmuir trough. *Langmuir* **1993**, *9*, 2426-2429.

44. Wang, W.; Moser, C. C.; Wheatley, M. A. Langmuir Trough Study of Surfactant Mixtures Used in the Production of a New Ultrasound Contrast Agent Consisting of Stabilized Microbubbles. *The Journal of Physical Chemistry* **1996**, *100*, 13815-13821.

45. Sirsi, S.; Pae, C.; Taek Oh, D. K.; Blomback, H.; Koubaa, A.; Papahadjopoulos-Sternberg, B.; Borden, M. Lung surfactant microbubbles. *Soft Matter* **2009**, *5*, 4835.

46. K. Bjerknes, J. U. Braenden, J. E. Braenden, R. Skurtveit, G. Smistad, I. Agerkvist Air-filled polymeric microcapsules from emulsions containing different organic phases. *Journal of*

Microencapsulation **2001***, 18*, 159-171.

47. Cui, W.; Bei, J.; Wang, S.; Zhi, G.; Zhao, Y.; Zhou, X.; Zhang, H.; Xu, Y. Preparation and evaluation of poly(L-lactide-co-glycolide) (PLGA) microbubbles as a contrast agent for myocardial contrast echocardiography. *Journal of Biomedical Materials Research Part B: Applied Biomaterials* **2005***, 73B*, 171-178.

48. Purdom, C. Program on History of Gelatin Breaks the Mold: Shedding Light on Familiar Dessert https://www.chicagotribune.com/news/ct-xpm-2001-04-10-0104100235-story.html (accessed Jul 14, 2020).

49. Matsuda, N.; Koyama, Y.; Hosaka, Y.; Ueda, H.; Watanabe, T.; Araya, T.; Irie, S.; Takehana, K. Effects of Ingestion of Collagen Peptide on Collagen Fibrils and Glycosaminoglycans in the Dermis. *Journal of Nutritional Science and Vitaminology* **2006***, 52*, 211-215.

50. Nomura, Y.; Oohashi, K.; Watanabe, M.; Kasugai, S. Increase in bone mineral density through oral administration of shark gelatin to ovariectomized rats. *Nutrition* **2005***, 21*, 1120-1126.

51. Levine, M.; Carpenter, D. C. Gelatin Liquefaction by Bacteria. *Journal of bacteriology* **1923***, 8*, 297-306.

52. Shevchenko, R. V.; Eeman, M.; Rowshanravan, B.; Allan, I. U.; Savina, I. N.; Illsley, M.; Salmon, M.; James, S. L.; James, S. E.; Mikhalovsky, S. V. The in vitro characterization of a gelatin scaffold, prepared by cryogelation and assessed in vivo as a dermal replacement in wound repair. *Acta Biomaterialia* **2014***, 10*, 3156-3166.

53. Ifkovits, J. L.; Devlin, J. J.; Eng, G.; Martens, T. P.; Vunjak-Novakovic, G.; Burdick, J. A. Biodegradable Fibrous Scaffolds with Tunable Properties Formed from Photo-Cross-Linkable Poly(glycerol sebacate). *ACS Applied Materials & Interfaces* **2009**, *1*, 1878-1886.

54. Kharaziha, M.; Nikkhah, M.; Shin, S.; Annabi, N.; Masoumi, N.; Gaharwar, A. K.; Camci-Unal, G.; Khademhosseini, A. PGS:Gelatin nanofibrous scaffolds with tunable mechanical and structural properties for engineering cardiac tissues. *Biomaterials* **2013**, *34*, 6355-6366.

55. Li, R.; Yau, T. M.; Weisel, R. D.; Mickle, D. A. G.; Sakai, T.; Choi, A.; Jia, Z. Construction of a bioengineered cardiac graft. *The Journal of Thoracic and Cardiovascular Surgery* **2000**, *119*, 368-375.

56. Nerurkar, N. L.; Elliott, D. M.; Mauck, R. L. Mechanics of oriented electrospun nanofibrous scaffolds for annulus fibrosus tissue engineering. *Journal of Orthopaedic Research* **2007**, *25*, 1018-1028.

57. Traut, R. R.; Bollen, A.; Sun, T.; Hershey, J. W. B.; Sundberg, J.; Pierce, L. R. Methyl 4-mercaptobutyrimidate as a cleavable crosslinking reagent and its application to the Escherichia coli 30S ribosome. *Biochemistry* **1973**, *12*, 3266-3273.

58. Jue, R.; Lambert, J. M.; Pierce, L. R.; Traut, R. R. Addition of sulfhydryl groups of Escherichia coli ribosomes by protein modification with 2-iminothiolane (methyl 4-mercaptobutyrimidate). *Biochemistry* **1978**, *17*, 5399-5406.

59. Lohcharoenkal, W.; Wang, L.; Chen, Y. C.; Rojanasakul, Y. Protein Nanoparticles as Drug Delivery Carriers for Cancer Therapy. *BioMed research international* **2014**, *2014*, 180549-12.

60. Suslick, K. S.; Grinstaff, M. W.; Kolbeck, K. J.; Wong, M. Characterization of sonochemically prepared proteinaceous microspheres. *Ultrasonics - Sonochemistry* **1994***, 1*, S65-S68.

61. Tabata, Y.; Ikada, Y. Synthesis of gelatin microspheres containing interferon. *Pharmaceutical research* **1989***, 6*, 422.

62. Akin, H.; Hasirci, N. Preparation and characterization of crosslinked gelatin microspheres. *Journal of Applied Polymer Science* **1995***, 58*, 95-100.

63. Vernon-Parry, K. D. Scanning electron microscopy: an introduction. *III-Vs Review* **2000***, 13*, 40-44.

64. Hayat, M. A. *Principles and techniques of scanning electron microscopy;* Van Nostrand Reinhold: New York, NY, 1978.

65. Goodhew, P. J.; Humphreys, J. *Electron Microscopy and Analysis;* CRC Press: GB, 2000.

66. Hunger, M.; Weitkamp, J. In situ IR, NMR, EPR, and UV/Vis Spectroscopy: Tools for New Insight into the Mechanisms of Heterogeneous Catalysis. *Angewandte Chemie International Edition* **2001***, 40*, 2954-2971.

67. Elwell, W. T.; Gidley, J. A. *Atomic-absorption spectrophotometry;* International series of monographs on analytical chemistry; Pergamon Pr: Braunschweig, 1966; Vol. 6.

68. Hook, F.; Rodahl, M.; Keller, C.; Glasmastar, K.; Fredriksson, C.; Dahlqvist, P.; Kasemo, B. Dissipative QCM-D technique: Interfacial phenomena and sensor applications for proteins, biomembranes, living cells and polymers. *Proceedings of the 1999 Joint Meeting of the*

European Frequency and Time Forum and the IEEE International Frequency Control Symposium *1999, 2*, 966-972.

69. Sigma-Aldrich. Gelatin product information https://www.sigmaaldrich.com/content/dam/sigma-aldrich/docs/Sigma/Product_Information_Sheet/2/g9382pis.pdf (accessed Dec 31, 2019).

70. Ma, X.; Bussonniere, A.; Liu, Q. A facile sonochemical synthesis of shell-stabilized reactive microbubbles using surface-thiolated bovine serum albumin with the Traut's reagent. *Ultrasonics sonochemistry* **2017**, *36*, 454-465.

71. Thermo Scientific. Zeba™ Spin Desalting Columns https://assets.thermofisher.com/TFS-Assets/LSG/manuals/MAN0011529_Zeba_Spin_DesaltCol_UG.pdf (accessed Dec 31, 2019).

72. Suslick, K. S.; Grinstaff, M. W.; Kolbeck, K. J.; Wong, M. Characterization of sonochemically prepared proteinaceous microspheres. *Ultrasonics - Sonochemistry* **1994**, *1*, S65-S68.

73. Nyquist, R. A.; Leugers, M. A.; Putzig, C. L. *Infrared Raman Spectral Atlas of Inorganic Compounds and Organic Salts: Handbook of Infrared and Raman Spectra of Inorganic Compounds and Organic Salts: Infrared Spectra;* Elsevier Science & Technology: St. Louis, 1996.

74. Ellman, G. L. Tissue sulfhydryl groups. *Archives of Biochemistry and Biophysics* **1959**, *82*, 70-77.

75. Rovers, T. A. M.; Sala, G.; van der Linden, E.; Meinders, M. B. J. Temperature is key to

yield and stability of BSA stabilized microbubbles. *Food Hydrocolloids* **2016**, *52*, 106-115.

76. Phan, H. T. M.; Bartelt-Hunt, S.; Rodenhausen, K. B.; Schubert, M.; Bartz, J. C. Investigation of Bovine Serum Albumin (BSA) Attachment onto Self-Assembled Monolayers (SAMs) Using Combinatorial Quartz Crystal Microbalance with Dissipation (QCM-D) and Spectroscopic Ellipsometry (SE). *PloS one* **2015**, *10*, e0141282.

77. Tzu-Yin Wang; Katheryne E. Wilson; Steven Machtaler; Jurgen K. Willmann Ultrasound and Microbubble Guided Drug Delivery: Mechanistic Understanding and Clinical Implications. *Current Pharmaceutical Biotechnology* **2013**, *14*, 743-752.

78. Tchuenbou-Magaia, F. L.; Al-Rifai, N.; Ishak, N. E. M.; Norton, I. T.; Cox, P. W. Suspensions of air cells with cysteine-rich protein coats: Air-filled emulsions. *Journal of Cellular Plastics* **2011**, *47*, 217-232.

79. Duggan, S.; O'Donovan, O.; Owens, E.; Cummins, W.; Hughes, H. Synthesis of mucoadhesive thiolated gelatin using a two-step reaction process. *European Journal of Pharmaceutics and Biopharmaceutics* **2015**, *91*, 75-81.